Selin Pars
BSc

CHARACTERIZATION OF A DAND5 P.R152H CONTROL-DERIVED IPS CELL LINE TO BE USED AS A TOOL FOR HEART DISEASE MODELING

Dissertation to obtain the Master degree in
Biochemistry for Health

Advisor: José A. Belo, PhD, CEDOC
Co-advisor: Graça Rosas, PhD, CEDOC

September, 2018

Selin Pars
BSc

CHARACTERIZATION OF DAND5 P.R152H CONTROL-DERIVED IPS CELL LINE TO BE USED AS A TOOL FOR HEART DISEASE MODELING

Dissertation to obtain the Master degree in
Biochemistry for Health

Advisor: José A. Belo, PhD, CEDOC
Co-advisor: Graça Rosas, PhD, CEDOC

Jury:

President:	Prof. Doutor António Sebastião Rodrigues
Main discussant:	Prof. Doutora José Eduardo Marques Bragança
Other members:	Prof. Doutor José António Henriques de Conde Belo
	Profª. Doutora Maria Teresa Nunes Mangas Catarino

CEDOC – Chronic Diseases Research Center - Nova Medical School
Universidade Nova de Lisboa

Funding: FCT (PTDC/BIM-MED/3363/2014)

September, 2018

Stem Cell Research 29 (2018) 202–206

Contents lists available at ScienceDirect

Stem Cell Research

journal homepage: www.elsevier.com/locate/scr

Lab Resource: Stem Cell Line

Generation and characterization of a human iPS cell line from a patient-related control to study disease mechanisms associated with DAND5 p.R152H alteration

Selin Pars[a,1], Fernando Cristo[a,1], José M. Inácio[a,1], Graça Rosas[a], Isabel Marques Carreira[b,c,d], Joana Barbosa Melo[b,c,d], Patrícia Mendes[e], Duarte Saraiva Martins[f], Luís Pereira de Almeida[g], José Maio[e], Rui Anjos[f], José A. Belo[a,*]

[a] Stem Cells and Development Laboratory, CEDOC, NOVA Medical School/Faculdade de Ciências Médicas, Universidade Nova de Lisboa, Lisbon, Portugal
[b] Cytogenetics and Genomics Laboratory, Faculty of Medicine, University of Coimbra, Coimbra, Portugal
[c] CNC.IBILI Consortium, University of Coimbra, Coimbra, Portugal
[d] CIMAGO - Center of Investigation on Environment Genetics and Oncobiology, Faculty of Medicine, University of Coimbra, Portugal
[e] Departamento Materno-Infantil, Centro Hospital do Algarve, EPE, Faro, Portugal
[f] Hospital de Santa Cruz, Centro Hospitalar Lisboa Ocidental, Lisbon, Portugal
[g] CNC - Center for Neurosciences & Cell Biology, University of Coimbra, Coimbra, Portugal

ABSTRACT

A *DAND5*-control human iPSC line was generated from the urinary cells of a phenotypically normal donor. Exfoliated renal epithelial (RE) cells were collected and reprogrammed into iPSCs using Sendai virus reprogramming system. The pluripotency, *in vitro* differentiation potential, karyotype stability, and the transgene-free status of generated iPSC line were analyzed and confirmed. This cell line can be exploited as a control iPSC line to better understand the mechanisms involved in *DAND5*-associated cardiac disease.

Resource table.

Unique stem cell line identifier	NMSUNLi002
Alternative name(s) of stem cell line	*iUC-DAND5_455/control*
Institution	*CEDOC, NOVA Medical School*
Contact information of distributor	José A. Belo, jose.belo@nms.unl.pt
Type of cell line	*iPSC*
Origin	Human
Additional origin info	*Sex: male* *Ethnicity: Caucasian*
Cell Source	*Exfoliated renal epithelial cells isolated from urine*
Clonality	*Clonal*
Method of reprogramming	*Transgene-free (Sendai virus vector)*
Genetic Modification	*NO*
Type of Modification	*N/A*
Associated disease	*N/A*
Gene/locus	*NM_152654.2:c.455G; DAND5 c.G455G; p.R152R*
Method of modification	*N/A*
Name of transgene or resistance	*N/A*
Inducible/constitutive system	*N/A*
Date archived/stock date	*January 2018*
Cell line repository/ bank	*N/A*
Ethical approval	*Approved by the Ethics Committee of NOVA Medical School (Protocol N° 13/2016/ CEFCM) and by the National Committee for Data Protection (CNPD, Permit N° 8694/ 2016).*

* Corresponding author.
E-mail address: jose.belo@nms.unl.pt (J.A. Belo).
[1] Equal authors.
https://doi.org/10.1016/j.scr.2018.04.015
Received 6 April 2018; Received in revised form 19 April 2018; Accepted 26 April 2018 Available online 28 April 2018

Resource utility

This *DAND5*-control iPSC line is essential in studying the disease related impairment in heart formation of DAND5 found in a previous study. This control cell line will allow to uncover the role of *DAND5* c.455 G > A variant in the molecular mechanisms of cardiomyocyte proliferation along with the previously established line.

Resource details

DAND5 is a Nodal antagonist that is involved in the correct left/ right body axis establishment during gastrulation (Belo et al., 2017). The heart is the first organ to be formed and the first organ to be af- fected by improper levels of Nodal signaling throughout embryo de- velopment. Several variants of different genes involved in this signaling pathway have been associated with Congenital Heart Disease (Deng et al., 2015). Recently, we have identified and functionally character- ized a c.455G > A *DAND5*-variant in a patient diagnosed with ven- tricular septal defect with overriding aorta, right ventricular hyper- trophy, and pulmonary atresia (a case of extreme tetralogy of Fallot phenotype) (Cristo et al., 2017a). The variant was inherited from the apparently healthy mother. To further study the impact of altered DAND5 proteins in molecular pathways that are involved in cardiac development and on cardiomyocyte behavior, we have generated and characterized the NMSUNLi001-A variant cell line, which has a het- erozygous non-synonymous variant in exon 2 of DAND5 gene (c.455G > A), causing an amino acid change of p.R152H in the func- tional domain of the DAND5 protein (Cristo et al., 2017b). However, to unveil the precise mechanism of how this variant affects early heart development, the generation of control iPSC lines is essential. Here, we generated and characterized a *DAND5* patient-related (father) control iPSC line that does not carry any alteration in the locus of the variant described in the NMSUNLi001-A cell line. This cell line will be utilized for disease modeling purpose. Hence, exfoliated renal epithelial (RE) cells were collected from urine sample collected from a healthy donor. After being grown during 7 days in culture, the RE cells were repro- grammed using CytoTune™-iPS 2.0 Reprogramming Kit (Life Technol- ogies, Invitrogen). The kit utilizes non-transmissible, non-integrating form of Sendai Virus (SeV) vectors that deliver four key transcription factors (SOX2, OCT3/4, c-MYC and KFL-4) to reprogram the somatic cells into a pluripotent state, and the iPSC colonies appeared 17 days after the delivery of the reprogramming factors. At this time, we ob- served that cells assumed typical stem cell morphology. To obtain homogeneous and clonal iPSCs lines, we manually picked and expanded several single cell-derived iPSCs colonies. Among those, one sub-clone that best displayed the ESC-like morphology (Fig. 1A) was chosen for further characterization. Firstly, after 27 passages in culture, DNA Sanger sequencing and karyotype analysis proved the genotype 455G in *DAND5* exon 2 (Fig. 1D), and the number (46, XY) and arrangement of chromosomes (Fig. 1C). We assessed the transgene-free status of the iPSC line by qPCR (Fig. 1E), confirming the clearance of the viral vectors. Since the cytoplasmic nature of SeV only allows the exogenous reprogramming vectors to be cleared after several passages, we used an early passage of iPSCs as a positive control. The pluripotency of the cells was analyzed by both fluorescence immunocytochemistry (Fig. 1F) and qPCR (Fig. 1B). We confirmed the expression of the key plur- ipotency factors OCT4, NANOG, and SSEA4 both at protein and mRNA level. At mRNA level, we additionally confirm the expression of pluripotency markers NODAL and SOX2. Embryoid body (EB) forma- tion assay was performed to assess the spontaneous differentiation potential of the iPSCs *in vitro*. From this assay, we assessed that the EBs cultured for 19 days expressed markers of the three germ layers: en- doderm, mesoderm, ectoderm, *i.e.*, alpha-fetoprotein (AFP), smooth muscle actin (SMA), tubulin beta-3 chain (TUBB3), respectively (Fig. 1G). Finally, STR analysis was performed showing that all the 16 loci tested matched (Table 1).

Materials and methods

Reprogramming of RE cells

RE cells were collected and expanded in culture. After ~4 days in culture, cells started to become evident and the medium was changed to REBM™ supplemented with REGM™ BulletKit (Lonza). When cells reached ~80% confluency, they were seeded on a 6-well plate and reprogrammed using CytoTune™-iPS 2.0 Sendai Reprogramming Kit (Life Technologies). At day 8 post-transduction, cells were passaged onto a 100 mm culture dish coated with Geltrex (Gibco, Thermo Fisher Scientific) and the next day medium was changed to Essential 8™ (E8) Flex medium, replaced until the iPSCs have emerged. 17 days post-transduction, colonies that best display an ESC-like morphology were picked and expanded with daily renewal of the E8 Flex medium.

Sequencing

To confirm the absence of the c.455G nucleotide in the established *DAND5*-control cell line, genomic DNA was extracted using ISOLATE II Genomic DNA kit (Bioline). Then, using the primers indicated in Table 2, exon 2 of *DAND5* was amplified by PCR and purified using NZYGelpure kit (NZYTech). Sequencing was conducted by STAB VIDA (http://www.stabvida.com/).

RNA extraction and real time qRT-PCR

The clearance of SeV transgenes and the expression of pluripotency markers OCT4, NANOG, SSEA4 (primers listed in Table 2) were carried out using Direct-zol™ RNA MiniPrep (Zymo Research). Subsequently, reverse transcription and qRT-PCR were performed.

Embryoid body formation assay

Embryoid bodies (EBs) consisting of approximately 2000 iPS cells/ 20 μl drop in Essential 8™ (E8) medium with 4 mg/ml polyvinylalcohol and RevitaCell™ Supplement (Thermo Fisher Scientific) were generated using hanging drop method. After 2 days, EBs were suspended in 50% E8 medium and 50% differentiation medium (DMEM with 20% FBS, Pen/Strep, NEAA, 2 mM L-glutamine, and 0,1 mM β-mercaptoethanol) and grown 3 more days. At day 5, EBs were placed on 24-well-plate with differentiation medium changes every other day. By day 19, EBs were fixed with 4% formaldehyde and the immunocytochemistry as- sayed for the three germ layers AFP, SMA and TUBB3.

Fluorescent immunocytochemistry (ICC)

Cells were fixed with 4% paraformaldehyde, permeabilized, blocked and incubated with primary and secondary antibodies (listed in Table 2) overnight at 4 °C. Prior to image acquisition, DAPI was used to stain DNA. All fluorescent images were acquired with confocal microscopy.

Karyotyping

Chromosome analysis was performed using GTG high resolution banding technique, according to standard procedures with a minimum of 10 metaphase spreads analyzed. Analysis of GTG-banded chromo- somes was performed at a resolution of 400 bands per haploid genome and karyotypes were established according to the International System for Human Cytogenetic Nomenclature (ISCN 2016).

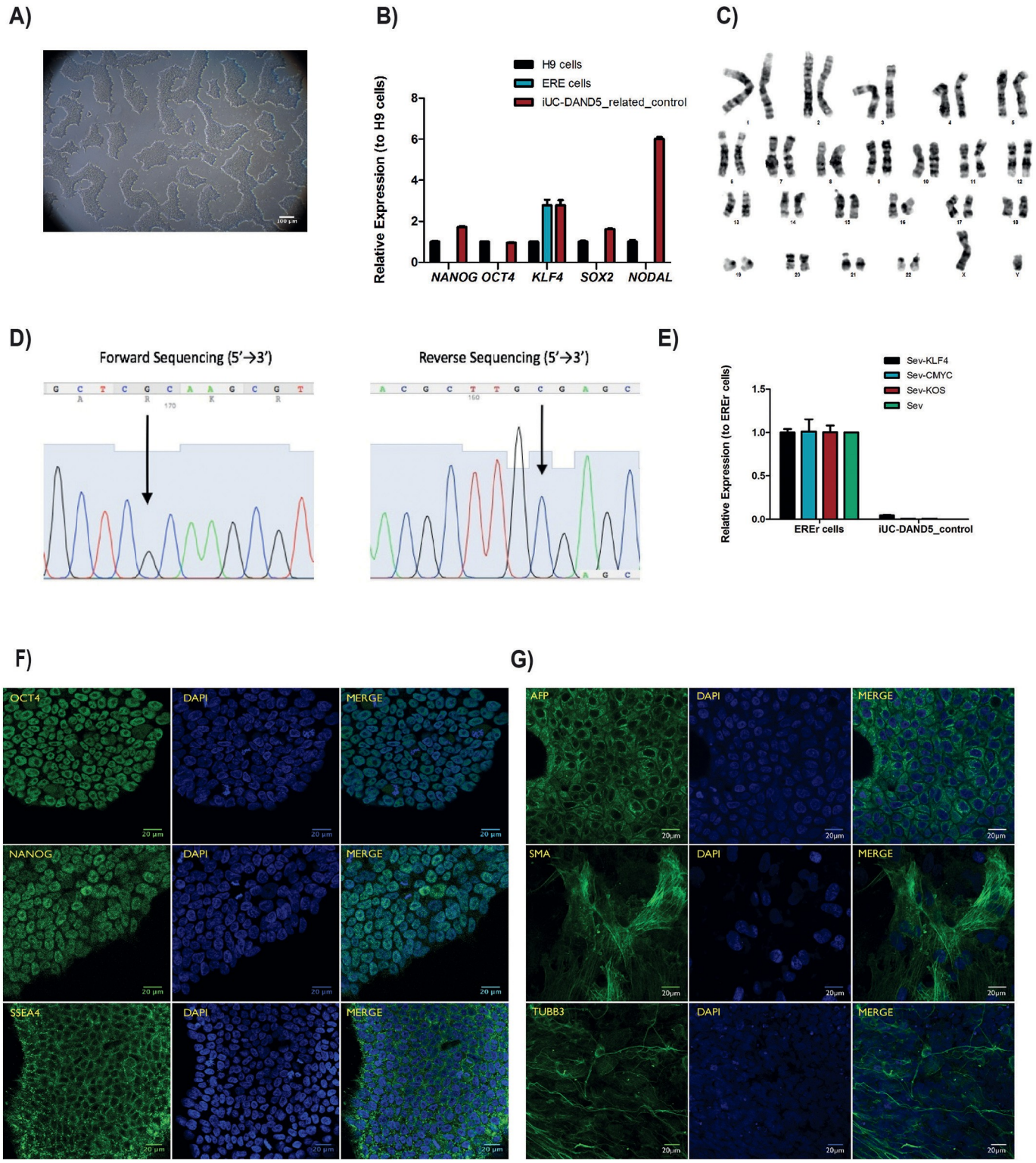

Fig. 1. Characterization of the iUC-DAND5_455/control iPSC line. A. Morphology of the iUC-DAND5_455/control line. B. mRNA expression levels of endogenous pluripotency markers in H9 cells (Black - positive control), ERE cells (Blue) and iUC-DAND5_455/control line (Red). CT-values were normalized to the geometric mean of the two housekeeping genes GAPDH and β-actin and with H9 human embryonic stem cell line as reference (set to 1). C. Karyotype of representative metaphase showing normal 46 chromosomes (XY). D. DNA sequence confirming the normal homozygous c.455G genotype in the iUC-DAND5_455/control line. E. Absolute quantitative real-time PCR showing absence of the vectors and the exogenous reprogramming factor in iPSCs (right) and presence of the reprogramming factors in the EREr control cells (left). F. Immunodetection of pluripotency markers of iUC-DAND5_455/control line. G. Immunofluorescence analyses of in vitro differentiation of EBs using specific antibodies against the endodermal marker α-fetoprotein (AFP), ectodermal marker βIII-tubulin (TUBB3) and mesodermal markers α-smooth muscle actin (SMA). Nuclei were stained with DAPI (scale bars = 20μm).

Table 1
Characterization and validation.

Classification	Test	Result	Data
Morphology	Photography	*ESC-like morphology*	Fig. 1, panel A
Phenotype	Immunocytochemistry	*Staining of pluripotency markers: Oct4, Nanog, SSEA4*	Fig. 1, panel F
	qPCR	*Expression of pluripotency markers: NANOG, OCT3/4, SOX2, KLF4 and NODAL*	Fig. 1, panel B
Genotype	Karyotype (G-banding) and resolution	*46XY, Resolution 400–500*	Fig. 1, panel C
Identity	Microsatellite PCR (mPCR)	*N/A*	
	STR analysis	*16 loci analyzed, all matching*	Supplementary Fig. S1 panel A
Mutation analysis (IF APPLICABLE)	Sequencing	*Homozygous (G > G)*	Fig. 1, panel D
	Southern Blot OR WGS	*N/A, Non-integrating reprogramming methodology*	
Microbiology and virology	Mycoplasma contamination	*Mycoplasma-free culture*	Supplementary Fig. S1 panel B
Differentiation potential	Embryoid body formation	*Proof of formation of three germ layers from Embryoid bodies: α-fetoprotein (AFP), βIII-tubulin (TUBB3), α-smooth muscle actin (SMA).*	Fig. 1, panel G
Donor screening (OPTIONAL)	HIV 1 + 2 Hepatitis B, Hepatitis C	*N/A*	N/A
Genotype additional info (OPTIONAL)	Blood group genotyping	*N/A*	N/A
	HLA tissue typing	*N/A*	N/A

Table 2
Reagents details.

Antibodies used for immunocytochemistry/flow-citometry

	Antibody	Dilution	Company Cat # and RRID
Pluripotency Markers	*Rabbit anti-NANO*	*1:200*	*Abcam Cat# ab21624, RRID:AB_446437*
	Rabbit anti-OCT4	*1:400*	*Abcam Cat# ab19857, RRID:AB_445175*
	Mouse anti-SSEA4	*1:200*	*Abcam Cat# ab16287, RRID:AB_778073*
Differentiation Markers	*Mouse anti-Human TUBB3*	*1:400*	*Sigma-Aldrich Cat# T8660, RRID:AB_477590*
	Mouse anti-Human SMA	*1:600*	*Dako Cat# M0851, RRID:AB_2223500*
	Rabbit anti-Human AFP	*1:200*	*Dako Cat# A0008, RRID:AB_2650473*
Secondary antibodies	*Alexa Fluor 488-conjugated Donkey anti-Mouse IgG (H + L)*	*1:300*	*Jackson ImmunoResearch Labs Cat# 715–545-150, RRID:AB_2340846*
	Alexa Fluor 488-conjugated Donkey anti-Rabbit IgG (H + L)	1:300	Jackson ImmunoResearch Labs Cat# 711–545-152, RRID:AB_2313584

Primers

	Target	Forward/Reverse primer (5′-3′)
Elimination of Sendai Virus transgenes (qPCR)	*Sev*	*GGATCACTAGGTGATATCGAGC/ACCAGACAAGAGTTT AAGAGATATGTATC*
	Sev-KLF4	*TTCCTGCATGCCAGAGGAGCCC/AATGTATCGAAGGTG CTCAA*
	Sev-C-MYC	*TAACTGACTAGCAGGCTTGTCG/TCCACATACAGTCCT GGATGATGATG*
	Sev-KOS	*ATGCACCGCTACGACGTGAGCGC/ACCTTGACAATC CTGATGTGG*
Pluripotency Markers (qPCR)	*NANOG*	*CATGAGTGTGGATCCAGCTTG/CCTGAATAAGCAGATCCATGG*
	OCT3/4	*GACAGGGGGAGGGGAGGAGCTAGG/CTTCCCTCCAACCAGTTGCCCCAAAC*
	SOX2	*GGGAAATGGGAGGGGTGCAAAAGAGG/TTGCGTGAGTGTGGATGGGATTGGTG*
	KLF4	*ACCAGGCACTACCGTAAACACA/GGTCCGACCTGGAAAATGCT*
	NODAL	*GGGCAAGAGGCACCGTCGACATCA/GGGACTCGGTGGGGCTGGTAACGTTTC*
House-Keeping Genes (qPCR)	*GAPDH*	*CTGGTAAAGTGGATATTGTTGCCAT/TGGAATCATATTGGAACATGTAAACC*
	β-actin	*GCAAAGACCTGTACGCCAAC/AGTACTTGCGCTCAGGAGGA*
Mycoplasma detection	*Pair 1*	*CTGCAGATTGCAAAGCAAGA/CCTCCTTCTTCACCTGCTTG*
	Pair 2	*GGCGAATGGGTGAGTAACACG/CGGATAACGCTTGCGACCTATG*
Targeted mutation analysis/sequencing	*DAND5 exon 2*	*GGAAGTGGACAGGTGATTATCC/CAC GTCTTTCTTGGTCCATCTC*

Mycoplasma contamination test

The sterility of the iPSC culture from mycoplasma was verified by PCR using the primers in Table 2.

STR analysis

iUC-DAND5_455/control cells and the corresponding ERE cells were authenticated by STR analysis performed by STAB VIDA (http://www.stabvida.com/).

Supplementary data to this article can be found online at https://doi.org/10.1016/j.scr.2018.04.015.

Author contributions

Conceived and designed the experiments: FC, SP, JMI, JB; Diagnosis of patients: PM, JM, RA; Patient recruitment, sample collection and

clinical data collection: FC, JMI, PM, JM, RA, DM; Analyzed thedata: FC, JMI, GR, JB; Performed the experiments: SP, FC, JMI, GR; Karyotype experiment and analysis: IMC, JBM, LPA; Contributed to writing the manuscript: SP, FC, JMI and JB. All authors read and approved the final manuscript.

Ethical statement

All the experimental protocols were approved by the Ethics Committee of the NOVA Medical School (Protocol N.°13/2016/CEFCM) and by the National Committee for Data Protection (CNPD, Permit N.° 8694/2016), according to European Union legislation. Written in- formed consent was obtained from patient guardian prior to sample collection.

Acknowledgements

We would like to thank the patient and their guardians for their generous donation of the urine sample used in this study. We also would like to thank Ana Jardim for technical support in karyotype analysis. This work was supported by Fundação para a Ciência e a Tecnologia (PTDC/BIM-MED/3363/2014). iNOVA4Health - UID/ Multi/04462/2013, a program financially supported by Fundação para a Ciência e Tecnologia/Ministério da Educação e Ciência, through na- tional funds and co-funded by FEDER under the PT2020 Partnership Agreement is acknowledged.

References

Belo, J., Marques, S., Inácio, J., 2017. The role of Cerl2 in the establishment of left-right asymmetries during axis formation and heart development. J. Cardiovasc. Dev. Dis. 4, 13.

Cristo, F., Inácio, J.M., de, Almeida S., Mendes, P., Martins, D.S., Maio, J., Anjos, R., Belo, J.A., 2017a. Functional study of DAND5 variant in patients with congenital heart disease and laterality defects. BMC Med. Genet. 18.

Cristo, F., Inácio, J.M., Rosas, G., Carreira, I.M., Melo, J.B., de, Almeida L.P., Mendes, P., Martins, D.S., Maio, J., Anjos, R., Belo, J.A., 2017b. Generation of human iPSC line from a patient with laterality defects and associated congenital heart anomalies carrying a DAND5 missense alteration. Stem Cell Res. 25, 152–156.

Deng, H., Xia, H., Deng, S., 2015. Genetic basis of human left-right asymmetry disorders.

ACKNOWLEDGEMENTS

I would firstly like to thank my thesis advisor Prof. José António Belo for the opportunity he provided for me to work in Stem Cells and Development Laboratory, CEDOC. He was always reachable and supportive during the time I was working on my thesis in his lab.
I am also profoundly grateful to Dr. Fernando Cristo for his support and expertise in the lab, as well as his valuable recommendations and input in my thesis. Dr. Graça Rosas has helped me from the beginning even in the busiest working days, and I am very thankful for the time she spent to teach me laboratory techniques and her handy advices in the lab.
I would also like to thank to Dr. José Manuel Inácio for his support and helpfulness. The rest of the Stem Cells and Development Lab, and the whole CEDOC family were also very welcoming and I appreciate all their help.
Lastly, I would like to express my gratitude to my parents and my partner, for their endless encouragement and support. I could not have completed this work without them. Many thanks!

Selin Pars

ABSTRACT

Congenital heart diseases (CHDs) and associated laterality defects are a major health concern and 1,35 million people are diagnosed with CHDs each year worldwide. The complexity of heart development and the hurdles to investigate the disease phenotypes make it challenging to identify the underlying causes of CHDs.

DAND5 is the human homologue of mouse Cerl-2 gene that codes for a protein involved in regulating the Nodal signalling pathway by antagonizing the Nodal protein in the node and inhibiting the Nodal signaling in the right lateral plate mesoderm (R-LPM). In a previous study, a new DAND5 heterozygous nonsynonymous variant c.455G>A was identified and linked to the risk of disease in two patients with CHDs arising from laterality defects. In order to model the phenotype of the patients with the variant c.455G>A, a human iPSC line was previously generated and characterized (Cristo *et al*., 2017).

In this work, we characterized a *DAND5*-control iPSC line from a healthy male donor (without the variant) to serve as control for the DAND5 c.455G>A line.

The characterization was based on the detection of pluripotency markers at gene- and protein level, and *in vitro* differential potential. Short tandem repeats (STR) analysis has used to prove the genetic identity of the ERE cells and the reprogrammed iPSCs. Karyotyping of the iPSCs after ≥20 passages has shown the stability of the highly proliferating iPSCs. Additionally, *Mycoplasma* detection test showed the sterility of the cell culture.

This control cell line will be compared to the DAND5 variant c.455G>A cell line to further exploit our knowledge on the consequences of the variant in the phenotypes of the patients (disease modelling) and more precisely in the modulation of cardiomyocyte proliferation (possible therapy).

RESUMO

As doenças cardíacas congênitas (DCC) e os defeitos de lateralidade associados são uma das principais preocupações de saúde e 1,35 milhões de pessoas são diagnosticadas com DCC a cada ano em todo o mundo. A complexidade do desenvolvimento do coração e os obstáculos para investigar os fenótipos da doença tornam difícil identificar as causas subjacentes das DCC.

O gene *DAND5* é o homólogo humano do Cerl-2 de camundongo que codifica uma proteína envolvida na regulação da via de sinalização Nodal antagonizando a proteína Nodal no nódulo e inibindo a sinalização Nodal na mesoderme da placa lateral direita (R-LPM). Em um estudo anterior, uma nova variante não-sinônima c.455G> A da *DAND5* heterozigótica foi identificada e vinculada ao risco de doença em dois pacientes com DCC decorrentes de defeitos de lateralidade. Para modelar o fenótipo dos pacientes com a variante c.455G> A, uma linha iPSC humana foi previamente gerada e caracterizada (Cristo et al., 2017).

Neste trabalho, caracterizamos uma linha iPSC de controle *DAND5* de um doador do sexo masculino sadio (sem a variante) para servir de controle para a linha DAND5 c.455G> A.

A caracterização foi baseada na detecção de marcadores de pluripotência a nível de genes e proteínas, e potencial diferencial in vitro. A análise de repetições curtas em tandem (STR) usou para provar a identidade genética das células ERE e das iPSCs reprogramadas. A cariotipagem das iPSCs após ≥ 20 passagens mostrou a estabilidade das iPSCs altamente proliferativas. Além disso, o teste de detecção de *Mycoplasma* mostrou a esterilidade da cultura de células.

Esta linha celular de controlo será comparada com a linhagem celular c.455G> A da variante DAND5, para explorar ainda mais o nosso conhecimento sobre as consequências da variante nos fenótipos dos doentes (modelação da doença) e, mais precisamente, na proliferação de cardiomiócitos (terapia possível).

ABBREVIATION LIST

ActRII: activin A receptor type 2
AFP: alpha fetoprotein
ALK4: activin A receptor type 1B
AoS: aortic stenosis
A/P: anterior/posterior
AP: arterial pole
APC: adenomatous polyposis coli
ARC105: mediator complex subunit 15
AS: aortic sac
ASD: atrial septal defect
AV: atrioventricular
AVE: anterior visceral endoderm
AVR: atrioventricular ring
AVSD: atrioventricular septal defects
A-P: anterior-posterior
BL-2: Biosafety Level 2
BSA: bovine serum albumin
Ccnd1: cyclin D1
cDNA: complementary deoxyribonucleic acid
Cerl-2: cerberus-like 2
CFC1: cripto, FRL-1, cryptic family 1
CHDs: Congenital Heart Diseases
CITED2: Cbp/p300 interacting transactivator with Glu/Asp rich carboxy-terminal domain 2
c-Myc: MYC proto-oncogene, bHLH transcription factor
CM: cardiomyocyte
CNS: central nervous system
CK1: casein kinase 1
Coarc: coarctation
Cripto: teratocarcinoma-derived growth factor 1
DAPI: 4′,6-diamidino-2-phenylindole
DAND5: Dan domain family member 5
DL: dextral looping
DMEM: Dulbecco's Modified Eagle Medium
DMSO: dimethyl sulfoxide
DNA: deoxyribonucleic acid
dNTP: deoxyribonucleotide triphosphate
DORV: double outlet right ventricle
Drp1: dynamin 1 like
DV: dorsoventral
DVL: dishevelled
EBs: embryoid bodies
EGF-FGF: epidermal growth factor-fibroblast growth factor
ERE: exfoliated renal epithelial
ESCs: embryonic stem cells

FBS: fetal bovine serum
FZL: Frizzled
GAPDH: glyceraldehyde 3-phosphate dehydrogenase
GATA4: GATA binding protein 4
GSK3ß: glycogen synthase kinase 3 beta
hESC: human embryonic stem cell
hiPSC: human induced pluripotent stem cell
ICC: immunocytochemistry
ICM: inner cell mass
iPSC: induced pluripotent stem cell
kDa: kilodalton
Klf-4: kruppel-like factor 4
KO: knock-out
KOS: Klf4–Oct3/4–Sox2
LDEV: lactose dehydrogenase elevating virus
Lefty1: left-right determination factor 1
Lefty2: left-right determination factor 2
LPM: lateral plate mesoderm
LR: left/right
LRP5/6: LDL receptor related protein 5
Nanog: Nanog homeobox
NEAA: non-essential amino acids
NF: nuclease-free
NKX2-4: NK2 homeobox 4
NKX2-5: NK2 homeobox 5
Nodal: nodal growth differentiation factor
NOTCH1: notch 1
NOTCH2: notch 2
Oct4: POU class 5 homeobox 1
PA: primitive atrium
PAHs: polycyclic aromatic hydrocarbons
PBS: phosphate-buffered saline
PCR: polymerase chain reaction
PDA: patent ductus arteriosus
PenStrep: penisilin/streptomycin
Pitx2: paired-like homeodomain 2
PLV: primitive left ventricle
Ppm1a: protein phosphatase, $Mg^{2+/}Mn^{2+}$ dependent 1A
PR: primary ring
PRV: primitive right ventricle
PS: pulmonary stenosis
PVA: polyvinyl alcohol
qPCR: quantitative polymerase chain reaction
RNA: ribonucleic acid
R-LPM: right lateral plate mesoderm
ROCK: rho-associated protein kinase
Rpm: revolutions per minute
RT: reverse transcriptase

RT-qPCR: real time quantitative polymerase chain reaction
SAR: sinoatrial ring
SeV: Sendai virus
SMA: smooth muscle actin
Smad2: SMAD family member 2
Smad3: SMAD family member 3
Smad4: SMAD family member 4
Sox2: sex determining region Y-box 2
SSEA4: stage-specific embryonic antigen-4
SSCs: somatic stem cells
STR: short tandem repeats
SV: sinus venosus
TBX1: T-box 1
TBX20: T-box 20
TCL/LEF: T cell factor/lymphoid enhancer factor
TGA: transposition of the great arteries
TGF-ß: transforming growth factor beta
TOF: Tetralogy of Fallot
TUBB3: class III ß-tubulin
VAR: ventriculoarterial ring
VP: venous pole
VSD: Ventricular Septal Defect
Wnt1: Wnt family member 1

INDEX

INDEX OF FIGURES

1. INTRODUCTION

1.1. Congenital Heart Diseases

Congenital heart diseases (CHDs) represent the abnormalities of the heart or the great vessels at birth, which accounts for 9 of 1,000 live births globally (Linde, Van Der *et al.*, 2011). This translates into an annual number of 1.35 million live births with CHDs out of 150 million births in the world. The symptoms of CHDs include shortness of breath, fatigue, heart murmur (Sun *et al.*, 2015). CHDs represent a wide range of heart defects that include ventricular septal defect, atrial septal defect, pulmonary stenosis, patent ductus arteriosus, tetralogy of Fallot, coarctation of aorta, and atrioventricular septal defect (Kumar V, Abbas AK, 2012). The most common subtype of CHDs is ventricular septal defect (VSD) on a global scale (Abdulkadir & Abdulkadir, 2016; Chelo *et al.*, 2016), followed by atrial septal defect (ASD) (Linde, Van Der *et al.*, 2011) (**Fig. 1.1**). Laterality defects, another type of CHD, display a prevalence of 1.1 in 10.000 live births (Lin *et al.*, 2014) and are caused by the improper left-right axis determination of the internal organs during the developmental stage. The disruption of the normal left-right axis establishment culminates in a variety of complex cardiac and extracardiac aberrations (Versacci *et al.*, 2018). Among these malformations, *situs inversus totalis* occurs when the internal organs develop as their complete mirror images, whereas in *situs ambiguous* (or *heterotaxy*) the internal thoracic or abdominal organs are assembled aberrantly (Vetrini *et al.*, 2016). However, whereas in *situs inversus* the prevalence of CHD is 3%, almost all the patients (90%) with heterotaxy also have complex congenital heart defects like pulmonary atresia/stenosis, transposition of the great arteries (TGA), double outlet right ventricle (DORV), ventricular septal defects (VSDs), atrial septal defects (ASDs), atrioventricular septal defects (AVSD), hypoplastic left heart, anomalous venous return and coarctation of the aorta (Mohapatra *et al.*, 2009).

The aetiology of CHDs is not well understood and characterized in most of the cases, nevertheless environmental, genetic and epigenetic factors together are known to play a role in the development of the disease. Environmental factors that of maternal origin include pregestational diabetes, pollakiuria, febrile illnesses, viral infections such as rubella and/or rubeola, influenza, alcohol consumption, cigarette smoking, use of medications, and teratogens (Chaix, 2016; Sun *et al.*, 2015). Moreover, recently, maternal

hypertension (Ramakrishnan *et al.*, 2015) and maternal exposure to polycyclic aromatic hydrocarbons (PAHs) were also been associated with the increased risk of CHDs (Li *et al.*, 2018). Among the genetic factors, chromosomal aberrations, single gene mutations or deletions are to be listed. Moreover, the patients can be categorized as syndromic and non-syndromic phenotypes. In Down, Edward, Patau, DiGeorge syndromes, chromosomal aneuploidies are responsible for the CHDs, whereas single gene deletions or mutations are the causative of Holt-Oram, Nooan, Allagille syndromes (Chaix, 2016). In the, case of non-syndromic patients, mutations in several genes, inherited according to Mendelian inheritance, have been shown as the cause of CHDs. Some of them include *NKX2-4, NKX2-5, CITED2, CFC1, GATA4, TBX1, TBX20, NOTCH1, NOTCH2* whose mutations are linked to CHDs (Deng *et al.*, 2014; Djordjevic *et al.*, 2015).
Additionally, since the major cause of mortality in laterality defects is related to complex CHDs, we can postulate that these defects can result from the disturbances of the left-right axis patterning. Therefore, variants in the genes involved in the establishment of the LR axis might also function as a risk factor or as a direct cause of CHDs (Ramsdell, 2005).

Due to the advances in early diagnostic methods and the availability of pediatric cardiac surgery, the mortality rate of the children born with CHDs decreased significantly over the last years. Between 1987-2005, the mortality of children with complex CHDs was reduced 67%, resulting in an increase of the median age of patients death by 15 years.
For the first time, the number of adults living with congenital heart diseases is higher than children. There are now an estimated 1.8 million adults in Europe with CHDs, and this number is expected to increase rapidly in the next years (Ávila *et al.*, 2014; Moons *et al.*, 2010). This brings several consequences, and adults with congenital heart disease, particularly those with moderate or complex disease, presented longer-term sequelae and face significant cardiac and noncardiac comorbidities and a shorted life expectancy that need be managed with special attention, care and differently than the pediatric patients. Moreover, these patients are an important adulthood problem with a high healthcare resource utilization and a significant source of global economic burden.

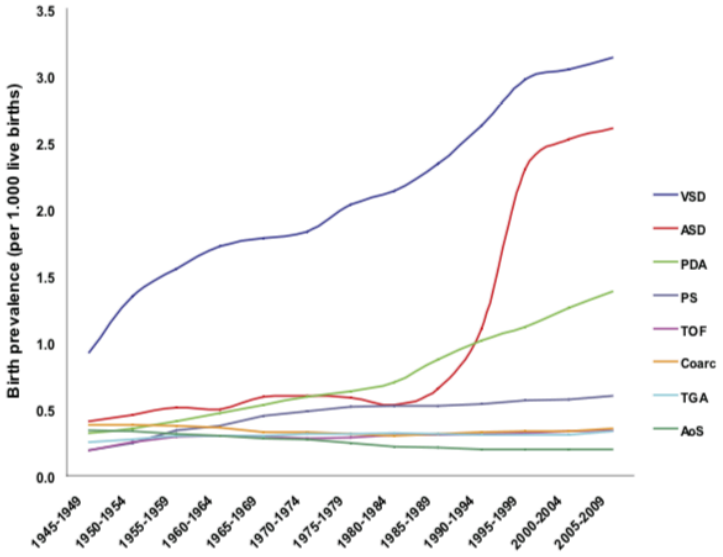

Figure 1.1. Prevelance of Congenital Heart Diseases (CHDs). The results include global data of birth prevelance over the period shown in the graph. AoS=aortic stenosis, ASD: atrial septal defect, Coarc: coarctation, PDA: patent ductus arteriosus, PS: pulmonary stenosis, TGA: transposition of the great arteries, TOF: tetralogy of Fallot, VSD: ventricular septal defect. (Obtained from Lin et al., 2014).

In order to discover therapeutic solutions for the CHDs and other cardiac diseases, an elaborate knowledge of the heart development is necessary. Moreover, since the heart have a limited regeneration capacity and heart transplantation is not always possible due to the inadequate organ supplies and immune rejection risk, the need for better understanding the cardiac disease mechanisms and the generation of desired amounts of cardiomyocytes is urgent.

Therefore, discovery of patient-specific iPSC raised the hopes that these cells could be used in multiple areas of research, disease modelling, drug screening, and translational therapies to serve as a solution to those patients. In the future, with the improvements of iPSC technology, functional cardiomyocyte generation may be scaled up and the the solution for cardiac diseases may be widely available.

1.2. An Overview of Heart Development

A functional heart requires the adequate pumping of the blood to all body parts, which is achieved by the coherence of the great vessels and heart chambers. The development of the human heart includes numerous steps that begins with the formation of mesoderm at

day 12 of gestation and is completed by the 8th week (Kumar V, Abbas AK, 2012). Initially, cardiac precursor cells that are located symmetrically in the splanchnic layer of the lateral plate mesoderm fuse in the midline and give rise to a primitive heart tube at day 17-19 of development in human and day 7 in the mouse embryo (Sylva, Hoff, Van den & Moorman, 2014). Afterwards, the heart tube elongates, bends and undergoes several looping steps, in order to provide the correct positioning of the atria and the ventricles. At the later stages with the addition of ectoderm-derived neural crest cells, specification and septation of the heart chambers is achieved, so that, the oxygenated and deoxygenated blood will precisely be present in separate chambers, allowing the proper functioning of the heart (Sieber-Blum, 2004).

All of these steps are strictly regulated and involving many genetic pathways that are highly conserved along the species (Sun & Kontaridis, 2018). Therefore, any impairment of these molecular pathways might disrupt the correct formation of the heart, resulting in congenital heart diseases (CHDs), the major cause of both infant morbidity and mortality in the first year of life (Fixler *et al.*, 2014; Gilboa *et al.*, 2016).

1.2.1. Embryonic Origins of the Heart

The journey of a human embryo begins with the fertilization of an egg cell with a spermatozoid to form a newly specialized cell called the zygote. The zygote undergoes repetitive cell divisions without gaining any size, being called morula. As the cell divisions of the sphere-shaped morula continue, the cells in the middle unequally take up nutrients due to the geometric nature of a sphere and therefore will need a wider surface area. At this embryonic stage, called blastocyst, a cavity in the middle part of the diving cells is formed, presenting an internal mass of cells called inner cell mass (ICM) or embryoblast and an outer cell layer called trophoblast (**Fig. 1.2A**) (Moore, Persaud & Torchia, 2016). Upon the implantation of the embryo into the uterine wall, trophoblast cells will undergo proliferation and differentiation and their lineages will mainly give rise to the extraembryonic tissues such as placenta (Silva & Serakides, 2016). The cells that make up the ICM will then differentiate into hypoblast (or primitive endoderm) and epiblast, forming a structure called bilaminar embryonic disc (**Fig. 1.2B**). The hypoblast will contribute to the extraembryonic tissues, whereas the epiblast contains pluripotent

cells that will form the three germ layers (i.e. endoderm, mesoderm, and ectoderm) and the germ cell lineage (Roode *et al.*, 2012).

At this stage, the epiblast and hypoblast cells of the bilaminar embryonic disc appear as a flat disc (Fig. 1.2B). Later on, at the midline of the embryonic disc, a structure called primitive streak will form, marking the first morphological sign of the gastrulation process.

The primitive streak also determines the anterior-posterior (A/P) axis of the embryo, a process that begins by the implantation of the blastocyst into the uterus. Upon implantation, in mice, the epiblast cells and the extraembryonic lineages (trophectoderm and primitive endoderm) undergo a series of proliferation and form an egg cylinder (Beddington e Robertson, 1999; Morris *et al.*, 2012). Once the egg cylinder is formed, the epiblast is positioned at the distal part of the embryo, whereas the extraembryonic ectoderm, derived from trophectoderm, is located at the proximal part. Around E5.5, primitive endoderm-derived anterior visceral endoderm (AVE) cells at the distal part of the embryo move unilaterally towards the anterior of the embryo and defines the point where the head will form (Srinivas, 2004). At the same time, the dorsoventral (DV) axis is specified according to the proximal-distal axis of the implantation site (Ferguson, 1996; Meinhardt, 2015). So, after implantation, the future A/P axis is marked anteriorly by the polarization of the head primordium and posteriorly (tail) by the appearance of the primitive streak, while the prospective DV axis is defined by the formation of the three germ layers, the endoderm marking its ventral side and the ectoderm being dorsal (Hamada & Tam, 2014; Hirokawa, Tanaka & Okada, 2009)
Once the A/P and DV axes are established, it is argued that the left-right (LR) axis is established consistently oriented relative to the dorsoventral and anterior.
The patterning of LR axis starts at gastrulation in a process involving the Nodal signalling pathway and a leftward flow of secreted molecules in the node that culminates in the creation of a LR-biased signal in this embryonic structure. Afterwards, this signal is transferred to the lateral plate mesoderm (LPM), and subsequently to internal organs for their asymmetric morphogenesis (Raya & Izpisúa Belmonte, 2006). The regulation of this process will be further elucidated in more detail in Section 1.2.

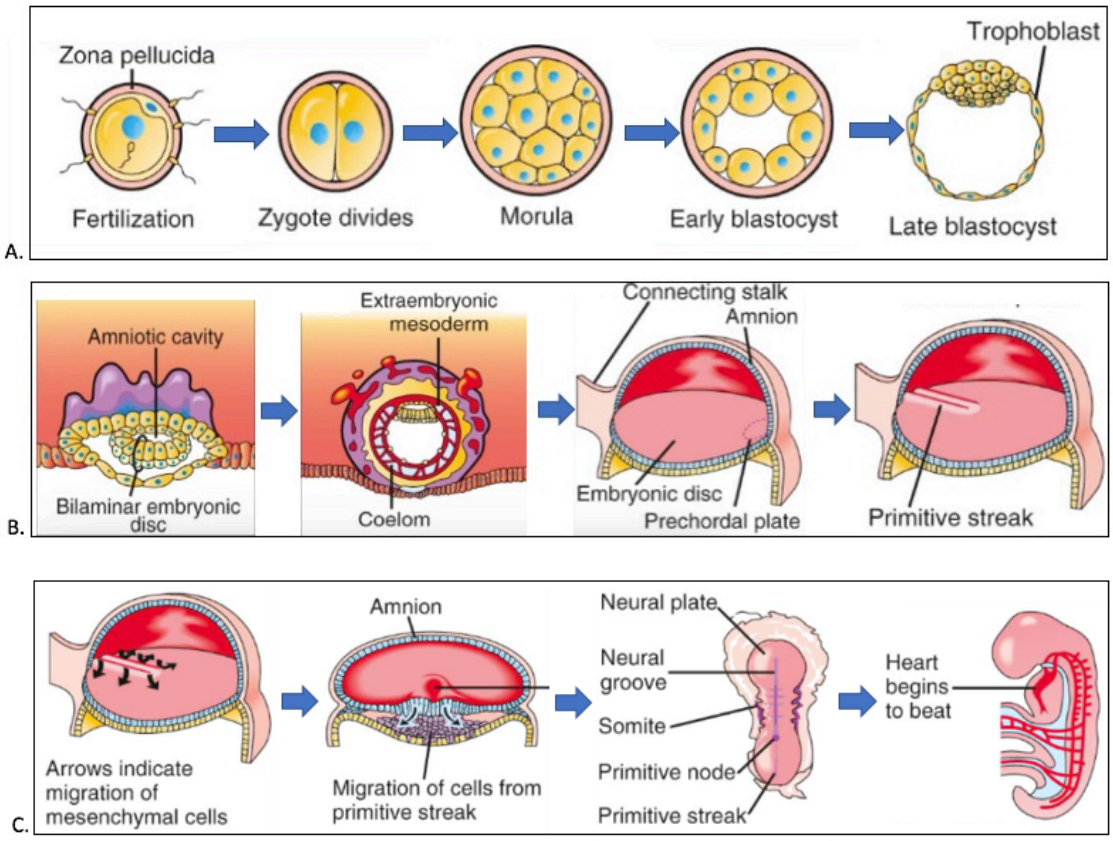

Figure 1.2. The developmental stages of the human heart formation. (Adapted from Moore, Persaud, Torchia, The Developing Human: Clinically Oriented Embryology, 2016).

1.2.2. Lateral Plate Mesoderm (LPM) Formation

At day 16 of development in humans and E6.5 in mouse, around the midline of the epiblast, the *primitive streak* forms in the posterior region of the embryo (**Fig. 1.2B**). This structure will continue from the midline of the bilaminar embryo to the caudal part. The cells around the primitive streak continuously divide laterally and cranially until they make up a lining above the hypoblast, forming two bilateral heart-forming regions (**Fig. 1.2C**). When the cells in the primitive streak stop dividing, we are left with three different layers that are solely derived from the epiblast; *ectoderm*, *mesoderm*, and *endoderm* (Schleich *et al.*, 2013). These three germ layers will give rise to the particular parts of the developing embryo. Ectoderm mainly will form the epidermis as well as the central nervous system (CNS), endoderm will line the gut and respiratory tract and mesoderm will give rise to the connective tissue and cardiovascular system.

The mesoderm can be divided into *somatic mesoderm*, *intermediate mesoderm*, and the *lateral plate mesoderm* (LPM). The somatic mesoderm cells will give rise to somites (Fig. 1.2C), which will form axial structures like skeleton and skeleton muscles and the intermediate mesoderm will form the kidneys and the gonads (Moorman, 2003; Musumeci *et al.*, 2015). The lateral plate mesoderm will differentiate into two distinct parts, the *somatic* LPM and the *visceral* LPM, which will originate the heart and some parts of the circulatory system like blood cells and blood vessels (Moorman, 2003).

1.2.3. Two Crucial Steps of the Heart Formation: Fusion of the Endocardial Tubes and Heart Looping

As the development of human foetus proceeds, in the visceral LPM, dorsal to the developing gut tube, the left and right *dorsal aortae* will appear, whereas the ventral *endocardial tubes* (or cardiogenic plate, **Fig. 1.3A**) will be formed ventral to the gut tube. The ventral endocardial tubes were initially thought to be symmetrical, but now we know that they are not completely symmetrical (Gittenberger-De Groot *et al.*, 2005). They are composed of crescent-shaped group of cells, where the first and second heart fields can be distinguished. The transition from mesodermal to cardiac progenitor cells requires the induction and specification of the splanchnic mesoderm into cardiac mesoderm, which is mediated by intrinsic signals from the primitive streak and from the surrounding tissues. Upon the fusion of the left and the right endocardial tubes, an arterial pole (AP) at the anterior and venous pole (VP) at the posterior will come into existence (Fig. 1.3A). During this time, the left and right parts of the ectoderm at the most outer layer of the embryo will band together and along with the somatic LPM, originating the *body wall*.

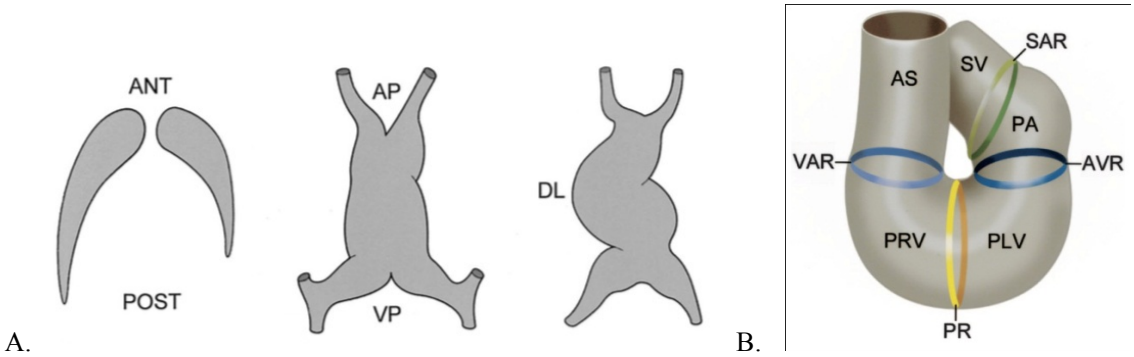

Figure 1.3. From the endocardial tubes to the chamber specification. A. Endocardial tubes emerge at the left and the right side of the embryo. At about day 23 of development they fuse and create one single endocardial tube. Venous pole (VP) at the posterior take up the blood and carry it to the arterial pole. The rightward (dextral) looping (DL) of the endocardial tube locates the heart chambers in their final positions, along with the subsequent septations. **B.** The spatial locations of sinus venosus (SV), primitive atrium (PA), primitive left- and right ventricles (PLV, PRV), and aortic sac (AS). Atrioventricular- and ventriculoarterial rings (AVR, VAR) will form the valves with the migration of endocardial cushions. (PR: primary ring, SAR: sinoatrial ring). (Adapted from Gittenberger-de Groot et al., 2005).

Around day 21 of development, the two endocardial tubes at the left and right side of the embryo will start to bind to each other and will fuse completely around day 23. Likewise, the two dorsal aortae will also fuse to be in contact with the endocardial tubes via the 1st and the 2nd aortic arches.

At this stage, the heart is still a long tube divided in the *sinus venosus* (SV), *primitive atrium* (PA), *primitive ventricle* (PV), *bulbus cordis*, and the *aortic sac* (AS) (**Fig. 1.3B**). SV will give rise to the right atrium, vena cavae, and the coronary sinus. PA and PV will give rise to the atria and the ventricles of the heart. Bulbus cordis will mostly form the right ventricle, whereas the aortic sac constructs the aortic arches.

The four-chambered heart will form after the looping of the heart. Before the looping, the aortic sac is at the superior part of the elongated tube and the sinus venosus in the inferior part. During the heart looping, the primordial atrium will end up being superior to the primordial ventricle, and at the same time, the bulbus cordis loops to the right side of the body (Fig 1.3B), forming the left and right ventricles together with the primordial ventricle.

Rightward cardiac looping is the first morphological indication of asymmetry in the vertebrate embryo and the mechanisms that drive this process are intrinsically related with the correct establishment of the LR axis during gastrulation. In turn, this correct left or right identity depends on a complex network of signals and molecules that are strictly regulated and maintained on the LPM in the form of Pitx2 expression, which will be described in Section 1.2 (Patel, Isaac & Cooke, 1999).

The incorrect looping of the endocardial tube at this stage is associated with some of the CHDs categorized as laterality defects such as sinus inversus totalis, heterotaxia (Schleich *et al.*, 2013).

1.2.4. Maturation of the Heart

Until this point, the positioning of the heart chambers is partially established. However, the septation and the rearrangement of the arteries need to occur for the heart to become a fully functional organ that pumps the sufficient blood to nourish all the body. Therefore, to achieve this maturation, firstly, the *atrioventricular* (AV) *canal* needs to be closed by *dorsal* and *ventral endocardial cushions*, followed by *left* and *right lateral cushions* and form the left and right AV canal (Fig 1.3B) (Sieber-Blum, 2004).

As mentioned before, primordial ventricle and the bulbus cordis will give rise to the left and the right ventricles. The looped parts of the endocardial tube, sinus venosus and primordial atria will form the right and the left atria. In addition to that, part of bulbus cordis will become the proximal aorta and the pulmonary trunk.

Once the four-chambered heart structure is established, the differentiating myocardium will be responsible for the conduction system instead of the peristaltic construction of the heart tube (Ya *et al.*, 1997).

The normal blood circulation will start with the entry of the venous blood from the body parts to the right atrium. Via the tricuspid valve, the venous blood will flow to the right ventricle and subsequently will be pumped to the lunges by pulmonary arteries. Simultaneously, the left atrium takes up the oxygenated blood from the pulmonary veins and pumps it to the left ventricle through the mitral valve. The oxygenated blood from left ventricle is then pumped to different body parts by aorta.

The conduction of the electrical impulses throughout the heart is achieved by nodes. Sinoatrial node, atrioventricular node, bundle of His and Purkinje fibers together orchestrate the conduction in the heart (Sánchez-Quintana & Yen Ho, 2003).
At later stages, coronary vascular formation of the heart will be accomplished by epicardium. The endothelial network that is derived from the epicardium will provide nutrition and oxygen for the heart itself (Tomanek, 2005).

Each and every step of the heart development should be correctly established, since their disturbance might result in congenital heart diseases.

1.3. Cardiac Left-Right Asymmetry

Vertebrates have an external bilateral symmetry along the left-right axis but present a left-right asymmetry of the internal organs (Levin, 2005). Although the first sign of left-right asymmetry occurs during the morphogenesis of the internal organs at the time of cardiac looping, the specification of the left-right axis takes place much earlier at gastrulation. At this time, cells that migrate from the primitive streak to the left and right parts of the embryonic midline are already exposed to different left and right patterning signals and will contribute to the distinct regions of the heart. These patterning signals, in turn, result from a number of events that are mainly controlled by the TGF-ß/Nodal signalling pathway and DAND5, a 20-kDa secreted growth factor with the ability to directly bind to Nodal and to inhibit its signalling pathways, play a critical role in this process (Hamada *et al.*, 2002; Zhou *et al.*, 1993).

1.3.1. Regulation of the Left-Right Axis Formation

The establishment of the left-right axis can be divided into three main steps; initial symmetry breaking at the node, the transfer of the LR-biased signal from the node to the LPM, and the left-right asymmetric positioning and morphogenesis of the visceral organs (Shiratori & Hamada, 2014).

The initial left-right symmetry breaking seems to originate in a structure called left-right organizer (node in amniotes; Kupffer's vesicle in Zebrafish). According to the widely accepted fluid flow model in symmetry breaking, the cells that are aligned along the LR organizer create a leftward flow by the motile cilia. This flow, namely nodal flow has been shown to be dependent on the motile cilia which reside in the mouse node (Nonaka *et al.*, 1998).

In **Figure 1.4**, the symmetry breaking mechanism in the vertebrate embryo is depicted. In the centre of the LR organizer, motile cilia are responsible to create the leftward nodal flow by rotating in a clockwise direction, whereas at the periphery, the immotile sensory cilia sense this flow in a mechanosensory way (Zinski, Tajer & Mullins, 2017). As a result of this leftward flow, the cells on the left part of the LR organizer degrade RNA of the *Cerl2* (*DAND5*), which results in the biased *Cerl2* expression on the right side of the LR organizer, resulting in the suppression of the Nodal signalling in the right side of the

embryo. The second step in the establishment of the LR axis involves the transference of the this LR biased signal to the left-LPM. The mechanism of the transduction of this signal is currently not known, but it is suggested that the peripheral cells of the LR organizer secrete Nodal ligands and the upon receptor binding, Nodal signalling will start in the left part of the LPM, where Nodal regulates its own expression by a positive-feedback mechanism. On the right side of the LPM, this signalling is disrupted by Nodal inhibitors, *Lefty1* and *Lefty2*. Lefty1 functions as a midline barrier that prevents Nodal to cross the midline and to induce bilateral expression of left-specific genes, whereas Lefty2 regulates the expression of Nodal in left LPM, restricting the intensity and area of Nodal signalling in a highly precise manner (Smith *et al.*, 2011).

After the LR biased signalling in the node has been accomplished and subsequently propagated through the left LPM, the signal must reach to the internal organs and be interpreted in order to initiate the asymmetrical morphogenesis of visceral organs.

The key gene responsible for this 3rd step of the LR axis formation is called *Pitx2*. As it can be seen in Fig. 1.4., *Pitx2* is initially expressed in the left LPM, and its expression is expanded throughout the whole left LPM.

The signalling of the asymmetry from the left LPM through to internal organs are achieved by *Pitx2* expression, which retains longer than other components of Nodal signalling pathway. During the next steps of cardiac development, when the primitive heart tube undergoes dextral looping to form the four-chambered heart, *Pitx2* expression is essential. Among the different isoforms of *Pitx2*, the cardiac-specific *Pitx2* (*Pitx2c*) is responsible for this cardiac looping, whose ectopic expression causes laterality defects of the heart such as situs inversus and cardiac isomerism (Liu *et al.*, 2001). Moreover, in the formation of atrioventricular canal by endocardial cushions, left-sided expression of *Pitx2* in the myocardium is detected. Additionally, *Pitx2c* expression was also shown in left atrium, left outflow tract, and interventricular myocardium (Ai *et al.*, 2006).

The abnormal expression of the *Pitx2* during the outflow tract rotation, as well as the leftward shifting of the heart tube might contribute to a number of congenital heart defects (CHDs) such as double outlet right ventricle (DORV), transposition of the great arteries (TGA), and ventricular septal defects (VSD). These findings suggest the multifunctional role of this gene in the cardiac left-right asymmetry.

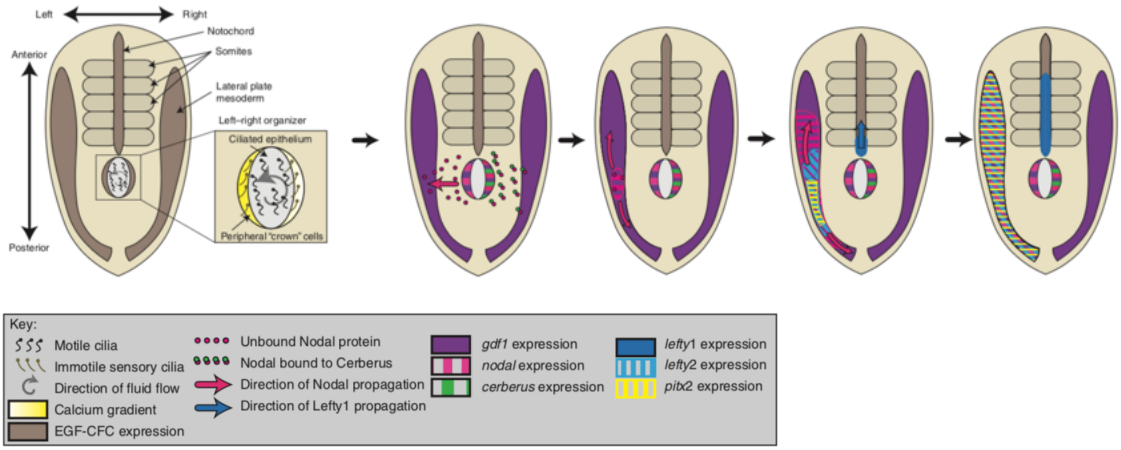

Figure 1.4. Nodal signalling pathway components in left-right symmetry breaking in vertebrates. (Adapted from Zinski, Tajer & Mullins, 2017).

1.3.2. Nodal Signalling and the Role of *DAND5*

The molecular cascade of the Nodal signalling pathway and its components are depicted in **Fig. 1.5.**

Nodal signalling is activated when the Nodal protein binds to a target cell through interaction to the ALK4 (serin-threonine kinase type I receptor) and ActRII (serin-threonine kinase type I receptor). Upon the receptor-ligand interaction and co-receptor involvement (Cripto or Cryptic), ALK4 phosphorylation at the cell membrane occurs. This leads to the subsequent phosphorylation of Smad2/Smad3, their association with Smad4 and the translocation of this complex to the nucleus. Here, the complex interacts with the transcription factor FoxH1 leading to activation of downstream target genes like *Nodal* itself (auto regulation), *Lefty2* and *Pitx2*, which is the main responsible for transducing the Nodal signaling afterwards (Hill, 2018; Shen, 2007).

The Nodal signalling pathway needs to be strictly regulated and this is achieved by the inhibitor Lefty1 and Lefty2 in the LPM and by the Cerl2/DAND5 protein at the node.

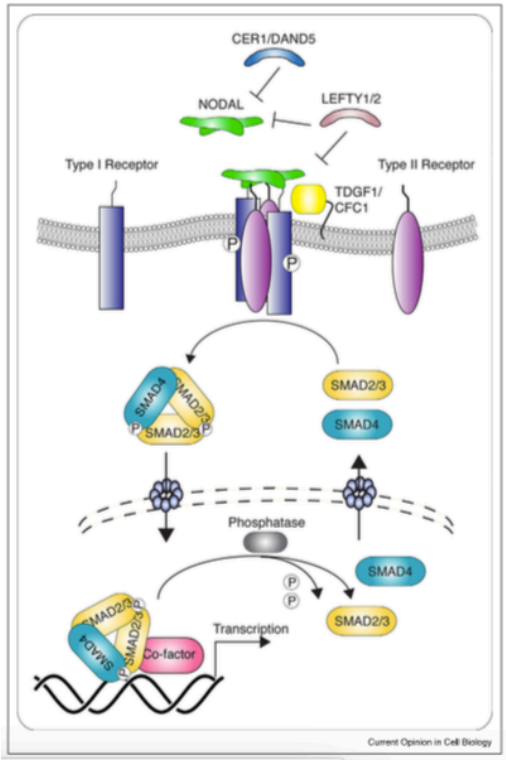

Figure 1.5. The components of Nodal signalling pathway. (Obtained from Hill, 2018)

Cerberus like 2 (Cerl-2) or *DAND5* gene in humans encodes a protein that belongs to the TGF-ß (transforming growth factor-ß) antagonists.

As a Nodal antagonist, the secreted Cerl-2 protein plays a crucial role in the determination of left-right asymmetry in mice (Marques *et al.*, 2004). At the mouse node, the asymmetric expression pattern of Cerl-2 represents the most immediate molecular response to the flow.

Prior to the appearance of the LR-biased signalling, the levels of Cerl-2 in peripheral crown cells are equal on the left and right side of the node. At this stage, the Nodal flow achieved by the motile cilia is very weak. As the leftward Nodal flow accelerates (E7.75), *Cerl-2* expression on the left side is downregulated, which breaks the symmetry of the Nodal signalling and creates a LR-bias in the node (E8.0).

The resulting Nodal signalling is therefore increased on the left side of the node (L>R), due to the relatively higher Nodal-inhibitory effect of *Cerl-2* on the right side.
At the 2/3 somite stage in mice, once the expression of *Cerl-2* in the right side of the node starts to become higher than the left side, Cerl-2 protein accumulates in the right side of the node, preventing the activation of Nodal cascade on the R-LPM (Saijoh *et al.*, 2003). When the velocity of the nodal flow becomes intense, it drives the translocation of the inhibitory Cerl-2 protein from the right to the left side of the node. This assumption is in agreement with the small size (20kDa) of this protein, which may render it easily transported (Inácio *et al.*, 2013). Until the 6-somite stage, the Cerl-2 protein remains in the left side of the node. By then, the signal starts to decrease and terminate.
As a summary, Cerl-2 is initially present in the right side of the mouse embryo, where it starts its Nodal inhibiting activity. Afterwards, the translocation of the Cerl-2 protein to the left LPM turns the Nodal signalling off (Oki *et al.*, 2009).

Cerl-2 is initially present in the right side of the mouse embryo, where it starts its Nodal inhibiting activity. Afterwards, the translocation of the protein to the left side of the embryo turns the Nodal signalling off (Inácio *et al.*, 2013).

The crucial role of Cerl-2 in the establishment of LR axis and consequent heart development is supported in the significant mortality rate due to the cardiac defects (including laterality defects) seen in *Cerl-2* knock-out (KO) mice. Moreover, the absence of *Cerl-2*, the only member of the Cerberus/DAN family expressed in the heart, observed in *Cerl-2* knock-out mice also results in a massive increase of the ventricular cardiac walls, without any laterality defect, suggesting that Cerl2 has a role in heart development other than establishing the left-right axis in mice (Araujo, Marques & Belo, 2014).

In fact, the hypertrophy of the ventricular walls in Cerl-2 KO mice were shown to be caused by increased levels of phospo-Smad2 that culminates in prolonged TGF-ß/Nodal signalling. Moreover, the ventricles of these mice also presented an increased mitotic index associated with an increased expression of Ccnd1, which functions as a cell cycle regulator. Considering that this signalling pathways regulates cardiac proliferation (in

addition to its roles in early cardiac specification, and differentiation), the presence of Cerl-2 seems to be specifically required in the heart to control the proliferation of cardiomyocytes through the control of TGF-B/Nodal signalling.

In addition to these findings, nuclear ß-catenin levels in the Cerl-2 KO mice was also shown to be increased. Wnt/ß-catenin signalling is also an important pathway that regulates proliferation and differentiation. Therefore, its upregulation highly affects the cardiomyocyte proliferation.

Overall, the lack of Cerl-2 in mice is associated with the dysregulation of both TGF-ß/Nodal, and Wnt/ß-catenin pathways, suggesting a possible role of Cerl-2 in cardiomyocyte proliferation.

Recently, the human homologue of *Cerl-2*, *DAND5* (Dan domain family member 5) was also studied and associated to the risk of developing CHDs in a cohort of CHD patients arising from defects during the establishment of the LR axis. In this study, conducted in our lab, a heterozygous nonsynonymous nucleotide variant c.455G>A, leading to a p.R152H a.a change in the functional domain of the DAND5 protein, has been found in two Caucasian patients with CHDs (Cristo *et al.*, 2017). Phenotypically, Proband 1 presents left isomerism, VSD with overriding aorta, and pulmonary atresia, whereas tetralogy of Fallot and pulmonary atresia was observed in Proband 2one of the patients (**Table 1.1)**. To get further insight in the consequences of the variant, a functional luciferase assay was performing and the results showed that the c.455G>A variant leads to a decreased activity of the DAND5 protein and consequently an increase in Nodal signalling (Cristo *et al.*, 2017). This means that during the embryonic development of the patients, NODAL and DAND5 protein binding might have been less efficient than normal, resulting in a reduced inhibitory effect of DAND5 in the node. Equally, NODAL could be expressed higher than its normal levels on the node and then in the LPM. It remains unknown if the excess level of NODAL was located on the left or right side of the LPM, however, from the patients' phenotypes, it can be concluded that an ectopic expression of *NODAL* (and *PITX2*) on the right-LPM might have occurred during the embryonic stage of the patients.

Altogether, these results link for the first time the reduced activity of a DAND5 variant with the human vulnerability for CHDs.

	Genotype	Protein alteration	Phenotype
Proband 1	*DAND5* c.455GA	DAND5 p.R152H	Left isomerism; VSD with overriding aorta; Pulmonary atresia
Proband 2	*DAND5* c.455GA	DAND5 p.R152H	Tetralogy of Fallot; Pulmonary atresia

VSD – ventricular septal defect
Wild type DAND5 refseq. - NM_152654.2

Table 1.1. Phenotypes of patients with *DAND5* variants. (Obtained from Cristo *et al*., 2017)

1.4. iPSC Technology

Due to the limitations of accessibility of some tissues in the body, such as the heart and the brain, there are diseases that cannot be easily studied. The use of stem cells represents a good solution to overcome this problem.

An important milestone in 1998 was achieved by the isolation and the cultivation of embryonic stem cells (ESCs) for the first time (Thomson, 1998). ESCs are pluripotent stem cells obtained at a very early stage of development that are capable of differentiating into all the cell types in an adult organism, and to proliferate indefinitely. Since ESCs are derived from oocytes and embryos their use in research and therapeutic approaches brings about ethical concerns with disputes about the onset of human personhood. To overcome these issues, the reprogramming of somatic cells to produce induced pluripotent stem cells has become, in the last years, the "gold standard" of stem cell research.

In 2006, for the first time, iPSCs from mouse fibroblast cells were generated *in vitro* by the groundbreaking work reported by Yamanaka (Takahashi & Yamanaka, 2006). A year after, the same approach was used to generate iPSC from adult human cells (Takahashi *et al.*, 2007). The researchers who developed this technique called reprogramming have used different combinations of 24 candidate genes to induce pluripotency in differentiated cells (Takahashi & Yamanaka, 2006) and after several attempts, they discovered that the combination of only four transcription factors (Oct4, Sox2, Klf4, c-Myc) were needed.

1.4.1. Reprogramming of iPSCs

Nowadays, it is possible to revert differentiated cells into an undifferentiated state by a technology called cell reprogramming (Yamanaka & Blau, 2010).

There is a vast amount of reprogramming strategies that have been developed in the last years. They can be distinguished as the integrative (retroviral and lentiviral vectors) and non-integrative methods (adenoviruses, Sendai virus vector, self-replicating episomal vectors), which depends on the integration of genetic material of the vector into the host genome. Integrative methods are more efficient, however, non-integrative methods are more advantageous because transgene integration bring safety concerns for therapeutic approaches. (Abou-Saleh *et al.*, 2018).

At the beginning of the iPSC technology, in the delivery of the pluripotency genes to the differentiated cells, retroviral vectors have been used (Stadtfeld & Hochedlinger, 2010).

Retroviral vectors are using RNA as genetic material and integrate to the host genome. Target cells that are transduced with retroviral vectors mostly depend on the exogenous expression of pluripotency genes and the persistence of the transgene expression in the host cells may cause tumour formation (Shao & Wu, 2010). Lentiviral vectors are another type of RNA based vectors, which are also integrative. They are more efficient than the retroviral vectors in the reprogramming of the differentiated cells and have a wider scale of the cell types that they can infect.

To overcome the drawbacks of the integrative methods, new delivery systems have been developed. They include the use of adenoviruses, Sendai virus vectors, and the self-replicating episomal vectors.

Adenoviruses are DNA viruses whose genetic material retains in the host cell as extrachromosomal element. Episomal vectors are advantageous due to their long expression time, however they have a low efficiency of reprogramming. Another type of non-integrative vector, Sendai virus (SeV), which is a negative-sense single stranded RNA virus, was shown to have a good efficiency in the generation of iPSC and allows exogenous expression of the pluripotency genes (Fusaki *et al.*, 2009). Although the genetic material of SeV does not integrate into the host genome, the transgenes are retained in the cytoplasm of the iPSCs and should be cleared after several passages. SeV vector penetrates to the host cell via the sialic acid receptors that are present on the cell membrane of a variety of animal species. As infection, replication and subsequent transcription occurs, (**Figure 1.6.**) the protein synthesis of the pluripotency factors begins.

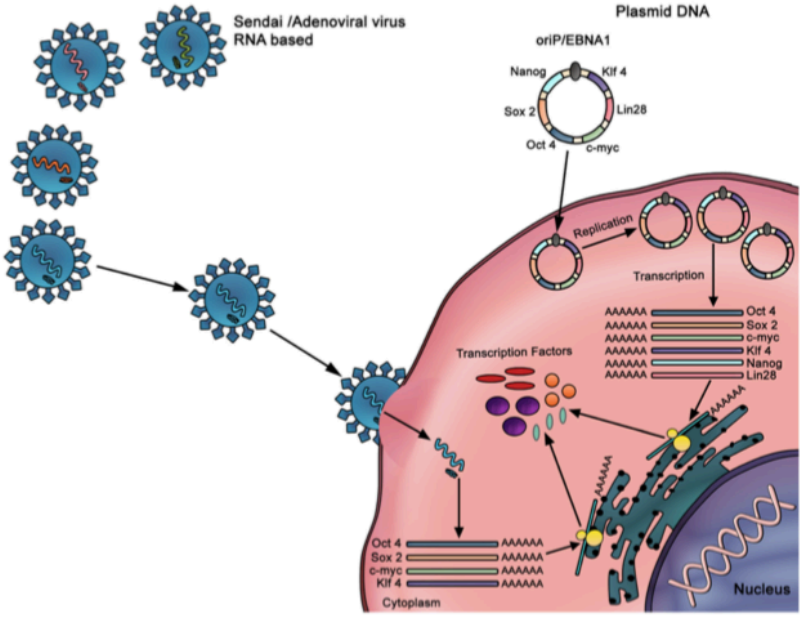

Figure 1.6. The delivery of the pluripotency genes into the target cell using non-integrative methods. (Abou-Saleh et al., 2018).

1.4.2. iPSCs: Generation and Characterization

IPSCs can be generated from different origins, using distinct reprogramming methods and initial cell sources.

Firstly, somatic cells from a patient are collected and cultured following specific protocols and under appropriate conditions (**Figure 1.7**).

The cell source can be from different origins such as fibroblasts, hepatocytes, B and T lymphocytes, keratinocytes, blood cells (cord blood cells, peripheral blood cells), and urine cells (Raab *et al.*, 2014; Singh *et al.*, 2015; Zhao *et al.*, 2013). The choice of the cell type will depend on several factors such as the availability of the cells, the reprogramming efficiency and non-invasive collection.

The accessibility and the reprogramming efficiency are some of the advantages of using fibroblasts, however, the risk of infection and chromosomal aberrations whilst taking biopsies are the drawbacks of using them. Peripheral blood cells are another type of cell sources, which is also easily accessible. When compared to fibroblasts, they require less effort in maintenance in the cell culture before the reprogramming experiments. Urine cells are readily available and accessible to be collected without the need of medical intervention (non-invasive).

After the establishment of the patient-derived somatic cell culture, they are transduced with the amenable vector that carries the pluripotency factors (Oct4, Sox2, Klf4, *c-Myc*). The newly reprogrammed colonies will be selected and further expanded to generate single origin iPSCs.

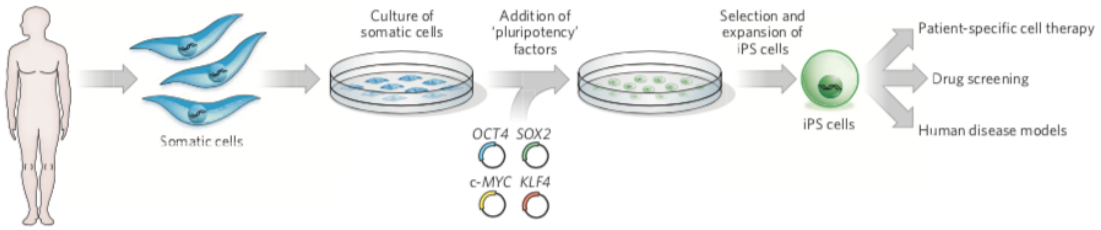

Figure 1.7. Processing of iPSC: from the patient to the therapeutics. (Yamanaka & Blau, 2010).

Once clonally selected and expanded, these cells can be used to accurately reflect the patients' disease phenotypes, not only for understanding the genetic mechanisms leading to the disease itself, but also for drug screening efforts aimed to the identification of potential personalized treatment therapies. This requires either the optimization of the current iPSC culturing protocols such as the maintenance of iPSC, the passaging type of the operator, and the preparation of the feeder cell layer are some of the variables that hinders reproducibility and need to be improved (Nagasaka *et al.*, 2017).

Once the iPSCs are successfully generated, they need to be characterized according to a set of well-established criteria.

Morphologically, iPSCs display a high nucleus to cytoplasm ratio and form compact colonies with defined borders (Wakao *et al.*, 2012). Additionally, as being pluripotent cells, they should express key pluripotency genes such as *Oct3/4*, *Sox2*, *Klf-4*, and *c-Myc* and be capable of self-renewal and differentiating into cells provenient of the three germ layers (Yu *et al.*, 2007). The proliferation rate of iPSCs are also similar to ESCs, ranging from 12-15 hours.

1.4.3. Patient-derived hiPSC-CMs

A number of disease modelling systems involving iPSCs are being pursued to model cardiac diseases, mainly cardiomyopathies (Kavyasudha *et al.*, 2018). Two examples of disease modelling of cardiomyopathies (in familial cardiomyopathy and Barth Syndrome) using hiPSC-CMs demonstrated the disease phenotype in the patient derived hiPSC-CMs *in vitro* (Wang *et al.*, 2014; Sun *et al*., 2012).

Another potential of patient-derived hiPSCs is in the replacement of the damaged cardiac tissue. This therapeutic approach aims to replace the lost cardiomyocytes in the heart tissue with the patient's own cells, which can be generated using chemically-defined medium *in vitro*. However, the *in vitro* differentiation of the CMs do not ensure the generation of mature CMs, which is desired for a potential transplantation (Dunn & Palecek, 2018).

1.5. Objectives

The development of the heart requires the interplay of many components in a living organism during the developmental stage. CHDs and/or laterality defects arise from the disruption of the normal cardiac development, whose aetiology is not fully understood. Considering the great numbers of affected patients from CHDs, there is a high burden on the shoulders of the patients themselves, and the health system all over the world.

The advances in the surgical procedures and technologies have made notable improvements for the CHD patients. In addition to that, the research in cardiac development has enabled us to obtain a wider knowledge in the field. However, the traditional research poses limitations and we need a more elaborate knowledge in the steps of cardiac development in order to explain the normal and disrupted development of the heart and subsequently discover therapeutic agents. Although some of the key genes that are responsible in cardiac development are well conserved in the model organisms that are commonly used, the use of human cells will provide a more direct and precise knowledge than the other model organisms.

Therefore, the objective of this study has been to establish a control iPSC line for the *DAND5* c.455G>A variant in order to shed light on the role of this gene in cardiomyocyte proliferation.

The research that originates the objective of this Master's thesis included the genetic screening of 38 patients diagnosed with CHDs. Two patients of this study population have been found to have a heterozygous non-synonymous variant in *DAND5*, which corresponds to the c.455G>A (Cristo *et al.*, 2017). This nucleic acid change which is located at the coding-region of *DAND5* (exon 2) results in an amino acid change at the p.R152H, which substitutes histidine for an arginine in the patients. The protein product of this variant has shown to have a significantly decreased Nodal-inhibitory activity in a Nodal-dependent luciferase assay (Cristo *et al.*, 2017). Any perturbation of DAND5 expression in the LPM might disrupt the Nodal signalling and because the location of the amino acid substitution is within the functional domain of the DAND5 protein, it is assumed that this variant might cause an abnormal Nodal activity in the node, which may have contributed to disrupted left-right axis patterning.

From the patients carrying the *DAND5* variant, iPSCs have been generated and one of them was characterized (Cristo *et al.*, 2017). As a straightforward and non-invasive

procedure, urine samples were collected from the patients and exfoliated renal epithelial cells were chosen as the cell source of the reprogramming. Also, the urinary cells possess a comperatively high reprogramming efficieny. The reprogramming was performed using Sendai virus (SeV), which is a non-integrating vector and introduces the key pluripotency genes (*Oct3/4, Sox2, Klf4, c-Myc*) to the target cells.

In this Master's study, based on the previous research of our lab, a DAND5-control human iPSC line was established and characterized using appropriate tools that determines the transgene-free status, pluripotency, *in vitro* differential potential, karyotype stability of the established cell line.

2. MATERIALS AND METHODS

2.1. Ethical Approval

All the experimental protocols were approved by the Ethics Committee of the NOVA Medical School (Protocol N.°13/2016/CEFCM) and by the National Committee for Data Protection (CNPD, Permit N.° 8694/2016), according to European Union legislation. Written informed consent was obtained from patient guardian prior to sample collection. The biological samples collected were anonymized to ensure the confidentiality and privacy of patients and data.

2.2. iPSC Source and Maintenance

Exfoliated renal epithelial (ERE) cells from a healthy Caucasian adult donor, without any alteration in the *DAND5* gene to serve as control cell line were previously collected and reprogrammed into iPSCs using the CytoTune™-iPS 2.0 Sendai Reprogramming Kit (Thermo Fisher Scientific) (Cristo, 2016).

After iPSCs generation, the cells were cryopreserved in Cryopreservation Medium (Thermo Fisher Scientific) or Essential 8™ Medium (Thermo Fisher Scientific) with 10% dimethyl sulfoxide (DMSO) at -150°C until further utilization.

2.3. Cell Culture Conditions of Human iPSCs

The culturing of the human iPSCs were carried out in Biosafety Level 2 (BL-2) laboratory, in an incubator exclusively used for stem cells, at 37°C, in atmospheric O_2 and 5% CO_2.

Essential 8™ Medium (Thermo Fisher Scientific) was used for the maintenance of the human iPSC in culture with the addition of ROCK-inhibitor (RevitaCell™ Supplement 100X, Thermo Fisher Scientific) in 1:100 dilution on the day of passage. Medium was changed every day. Cells were passaged every three or four days, when they reached 85% confluency, using TrypLE™ Select Enzyme 1X (Thermo Fisher Scientific). 6-well plates (Thermo Fisher Scientific) were used for the incubation of the cells along with Geltrex™ LDEV-Free hESC-qualified Reduced Growth Factor Basement Membrane Matrix (Thermo Fisher Scientific), if not otherwise indicated.

2.4. Characterization of Human *DAND5*-control iPSC Line

The workflow of the characterization of the generated iPSC line started with the sequencing analysis to confirm the lack of any nucleotide substitution in exon 2 of *DAND5* gene. After that, short tandem repeat (STR) analysis of the ERE cells (cell source) and the generated iPSCs confirmed that the somatic cells used for reprogramming and derivative stem cell line are genetically identical iPSCs after the reprogramming process.

Then, we tested the transgene-free status of the iPSCs by real-time quantitative polymerase chain reaction (RT-qPCR). Next, *Mycoplasma* test has been performed to prove the lack of *Mycoplasma* contamination of the culture medium and cells. Subsequently, in order to assess the pluripotency of the iPSCs, RT-qPCR and immunocytochemistry (ICC) assays were performed. In addition to these assays, embryoid body formation assay was used to test the *in vitro* differentiation potential of the iPSCs. Lastly, the chromosome stability of the iPSC cells, over 20 passages, was verified by the analysis of the karyotype.

2.4.1. Embryonic Stem Cell (ESC)-like Morphology

The generated iPSC line displayed ESC-like morphology; mainly being characterized by the high nucleus to cytoplasmic ratio, formation of the colonies with defined borders. The cells in culture have routinely been inspected under the microscope whilst changing the culture medium, and prior to cell passages.

2.4.2. DNA Sequencing

To confirm the absence of the c.455G nucleotide in the established *DAND5*-control cell line, genomic DNA was extracted using ISOLATE II Genomic DNA kit (Bioline). Then, using the primers indicated in Annex III, Table 1.4, exon 2 of DAND5 was amplified by PCR and purified using NZYGelpure kit (NZYTech) according to the PCR protocol in Annex I-1. Direct bidirectional DNA sequencing was conducted by STAB VIDA (http://www.stabvida.com/). The sequencing data was analysed using 4Peaks software v 1.8 and compared with consensus sequences obtained from the human genome databases in the online program BLAST (https://blast.ncbi.nlm.nih.gov/Blast.cgi).

2.4.3. Short Tandem Repeats (STR) Analysis

Genomic DNA from *DAND5*-control iPSCs and corresponding ERE cells were extracted using ISOLATE II Genomic DNA kit (Bioline) according to the manufacturer's instructions. The DNA elutions were conducted from ~1x10^6 cells. After the quality control procedure of the sample in agarose gel electrophoresis, DNA was amplified with multiplex PCR using PowerPlex 16 Kit. Analyzed loci are as follows: D351358, TH01, D21511, D18551, Penta E, D5S818, D13S317, D7S820, D16S539, CSF1PO, Penta D, Amelogenin, vWA, D8S1179, TPOX, FGA.

The sequencing of the DNA was performed using ABI 3100 DNA Analyser and the genotype analysis was done by GeneMarker HD software v 1.75. The steps after the extraction of the genomic DNA were executed by STABVIDA.

2.4.4. Transgene-free Status

Quantitative real time PCR was performed to assess the absence of Sendai virus (SeV) transgenes with primers suggested in the CytoTune-iPS 2.0 Sendai Reprogramming Kit (see Table 1.3. in Annex III). To do that, we used cDNA of the *DAND5*-control iPSCs at passage 29, diluted 1:5 and, cDNA from an early passage (4) of those cells as a positive control and cDNA from exfoliated epithelial renal cells as a negative control.

2.4.5. *Mycoplasma* Contamination Detection

Mycoplasma contamination was assessed by collecting Essential 8™ Medium from the iPSCs that were grown in cell culture. Afterwards, PCR was carried out with the primers named *Mycoplasma* and listed in Table 1.5, in Annex III. As a positive control, a sample contaminated with *Mycoplasma* was used, whereas the stock medium was used as a negative control.

2.4.6. RNA Extraction, cDNA Synthesis and qRT-PCR

Total RNA of approximately 1x10^6 cells was extracted and purified from control iPSC line, H9 human embryonic stem cell line as a positive control and exfoliated renal epithelial cells using TRIzol Reagent (Invitrogen) plus Direct-zol™ RNA MiniPrep kit (Zymo Research) according to the manufacturer's instructions.

After the total RNA was obtained from the iPSCs, cDNA synthesis was performed using 1000 ng RNA and with the RevertAid RT Reverse Transcription Kit (Thermo Scientific). PCR of cDNA synthesis were carried out at temperatures 65°C for 5', 42°C for 60', 72°C for 5', in C1000™ Thermal Cycler (BioRad) instrument. cDNA was then diluted 1:10, with nuclease-free water, and 2 µl were used to quantify by qRT-PCR the expression of the target genes. qRT-PCR was performed on an Applied Biosystems® 7500 Real-Time PCR machine and reactions were run with SYBR® Select Master Mix (Applied Biosystems). CT-values were normalized to the geometric mean of the two housekeeping genes GAPDH and β-actin and with H9 human embryonic stem cell (ESC) line as reference (set to 1).

2.4.7. Detection of Pluripotency Markers - Immunocytochemistry

ICC of the iPSCs was performed on Geltrex-coated cover slips in 24-well-plates, when the cells reached 50-60% confluency.

One day after, cells were initially washed with PBS and fixed with 4% formaldehyde for 30', then washed with PBS, permeabilized with PBS with 0,1% Triton-X-100 for 30' (this step was shortened to 7' for the cell surface protein SSEA4), blocked with blocking solution (BS: 0,4g BSA, 0,04 g NaN_3, 1,5g glycine in 200ml PBS) for 30' and incubated with primary antibodies (see Annex III) overnight at 4°C. In the next day, the cells were washed with BS, and incubated with secondary antibodies (see Annex III) overnight at 4°C. At day 3, cells were washed again with BS, incubated with 4',6-diamidino-2-phenylindole (DAPI) 1:1000 in PBS for 35' in dark, washed and kept in PBS.

Coverslips were then carefully picked and mounted on a microscope slide covered with Mowiol mounting media, and sealed with nail polish to fix the coverslips on the slides.

The images were immediately acquired in confocal microscope (LSM710, Zeiss) or widefield fluorescent microscope (Z2 Axio Imager, Zeiss).

Note: All the washing steps were repeated three times, 5 minutes each.

2.4.8. Detection of *in vitro* Differentiation Potential

The spontaneous differentiation potential of the iPSCs were analysed using the hanging drop method to generate embryoid bodies (EBs). After regular passaging, at D0, 2000

cells per 20µl were resuspended with EB formation media (4mg/ml PVA, RevitaCell™ Supplement 1X in Essential 8™ Medium, filtered). on 100 mm culture dish. In order to grow the EBs, a growth medium (DMEM with 20% FBS, 1% Glutamine, 1% NEAA, ß-mercaptoethanol and 1% Pen Strep) was previously prepared. At D2, the EB drops were suspended in Essential 8™ and EB growth medium (1:1). From D4, only EB growth medium was used to grow the cells. When the EBs were big enough, normally at D5, the EBs were manually picked and placed on cover slips coated with Geltrex on a 24-well-plate. Medium was changed every other day until the distinct cell types were observed under the microscope. Therefore, normally between days 19-21, the cells were fixed and the immunocytochemistry assay started as described above.

2.4.9. Karyotype Analysis

Karyotyping was performed according to the protocols from Laboratório de Citogenética e Genómica, Faculdade de Medicina da Universidade de Coimbra. Briefly, chromosome analysis was performed using GTG high resolution banding technique, according to standard procedures with a minimum of 10 metaphase spreads analyzed. Analysis of GTG-banded chromosomes was performed at a resolution of 400 bands per haploid genome and karyotypes were established according to the International System for Human Cytogenetic Nomenclature (ISCN 2016).

3. RESULTS

3.1. Morphology of *DAND5*-control iPSCs

After generation and clonal expansion of the *DAND5*-control iPSC line, the cells continued to display a typical small, round shape, and tightly packed ESC-like morphology with defined borders, a high nucleus/cytoplasm ratio with prominent nucleoli as presented in **Figure 3.1.**, suggesting that the generated iPSC lines were successfully reprogrammed.

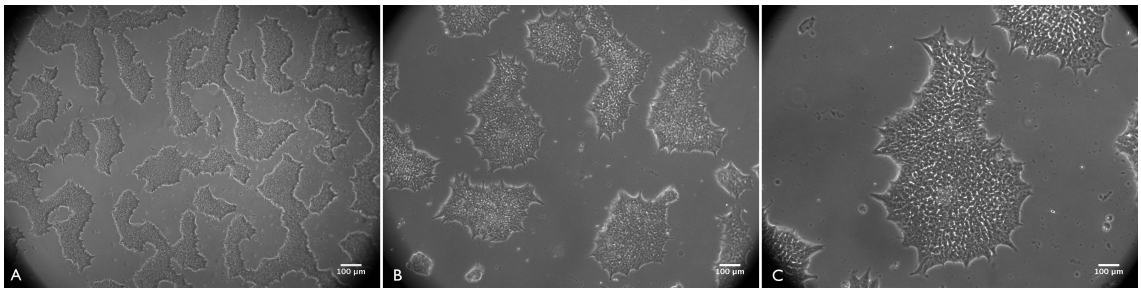

Figure 3.1. Generated *DAND5*-control iPSCs in culture. A. 5X, **B**. 10X, **C.** 20X. Characteristic iPSC properties are observable such as defined borders of the colonies, large nucleoli of the cells, and their round shape. The cells are at passage 27, and the image is acquired with a Zeiss Axiovert 40 CFL.

3.2. Sequencing Analysis of *DAND5* Exon2

The main purpose of this thesis was the establishment of a *DAND5*-control iPSC line. with a wild-type allele, G, in the position c.455 of the exon 2 of the *DAND5* gene to serve as control for the DAND5 c.455 G>A line generated before. Therefore, DNA Sanger sequencing confirmed the homozygous presence of the c.455G>G allele in the exon 2 of *DAND5* gene, corresponding to a R152R amino acid protein, in one clone of the iPSC line derived from the healthy control individual (**Figure 3.2**).

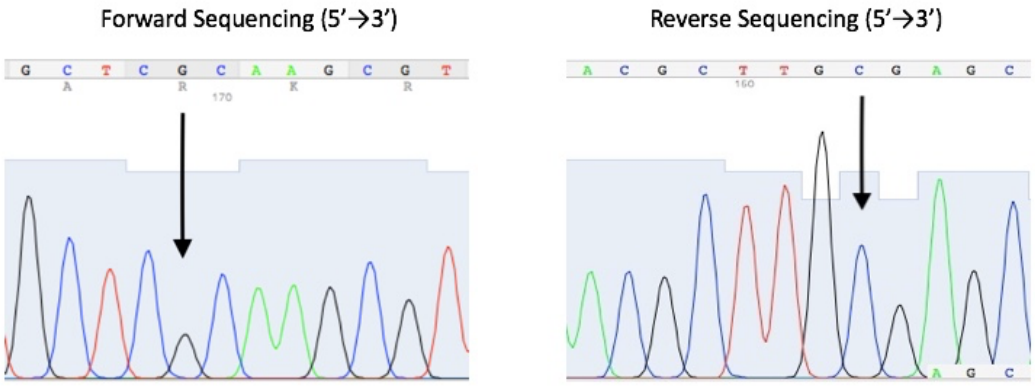

Figure 3.2. Forward and Reverse sequencing of *DAND5* exon2. DNA sequence confirming the normal homozygous c.455G genotype in the *DAND5*-control cell line. The arrow at the left image indicates the unaltered genotype 455G in the forward sequence, whereas the arrow at the right image shows the corresponding cytosine in the reverse sequence.

3.3. STR Analysis

Short tandem repeat (STR) analysis is a tool used to identify unknown samples based on the repeat number of nucleic acids in a number of different independent loci. The use of different loci increases the accuracy of the technique, since the probability of someone sharing the same repeat number will be less likely (McNamara-Schroeder *et al.*, 2006). For the characterization of this *DAND5*-control iPSCs line, 16 loci in donor cells (ERE cells) and the iPSCs have been compared to ensure the identity of the iPSCs after the reprogramming. The result, presented in the Fig. 3.3 showed that all the 16 loci from both alleles, in both samples have matched proving the genetic identity between both cell types.

PowerPlex 16 Loci	Sample UC13 (PG005)		Sample iUC13 7.37 (PG006)	
D3S1358	15	16	15	16
TH01	6	9	6	9
D21S11	30	33.2	30	33.2
D18S51	14	17	14	17
Penta E	7	10	7	10
D5S818	11	12	11	12
D13S317	13	14	13	14
D7S820	10	12	10	12
D16S539	12	12	12	12
CSF1PO	9	10	9	10
Penta D	12	12	12	12
Amelogenin	X	Y	X	Y
vWA	18	18	18	18
D8S1179	11	14	11	14
TPOX	8	8	8	8
FGA	19	20	19	20

Figure 3.3. STR analysis of the iPSC in comparison with the ERE cells. Sample UC13 represents the donor ERE cells, whereas Sample iUC13 7.37 represents the reprogrammed iPSCs. Listed numbers indicate the repeat number of each specified loci for both alleles, in each sample, whereas X and Y stands for the sex chromosomes.

3.4. Clearance of the Transgenes – Lack of Transgene Expression (qPCR)

The use of virus particles to reprogram the somatic cells present some safety issues concerning the integration of the virus genome in the host cells or the persistence of the virus in the cytoplasm of the cells. Thus, the proof of the transgene-free cell line is a standard procedure in our day to validate the cell line. The Sendai virus vector used in the reprogramming of the ERE cells into iPSCs in this work is a modified form of the wild type SeV, which is a transmissible and pathogenic RNA virus (Fujie. *et al.*, 2014). This modified version of the SeV lacks the fusion protein, which hinders the generation of the infectious particles in the transduced cells. Moreover, the functional mutations in several proteins of the virus facilitates the removal of the virus from the infected cells. Therefore, this system is non-pathogenic to humans and non-transmissible, does not integrate into the genome of the transduced cells and the transgenes of the SeV are expected to be diluted in the generated iPSCs after several passages in culture.

Even though the modified Sendai virus is non-pathogenic and non-transmissible, the expression of the pluripotency genes should only represent the endogenous expression of

those genes. Therefore, we evaluated the lack of the transgenes in the generated iPSC line by quantitative real-time PCR.

Since the SeV is a RNA-virus, after the extraction of the RNA from the iPSC, we synthetized cDNA to perform a qRT-PCR using primers that amplify Sendai virus-specific genes. Four different sets of primers have been used in the qRT-PCR experiment; SeV, KOS, Klf-4, and c-Myc. KOS consists of the human *Klf-4*, human *Oct3/*4, and human *Sox2*. According to the Fig. 3.4, the iPSCs, indicated as iUC-DAND5-control, presented a relative expression closer to zero relative to the ERE cells (used as negative control), for each gene tested. This result suggests that neither the SeV vector, nor the SeV-Klf4, SeV-c-Myc, SeV-KOS are present in the generated *DAND5*-control iPSCs.

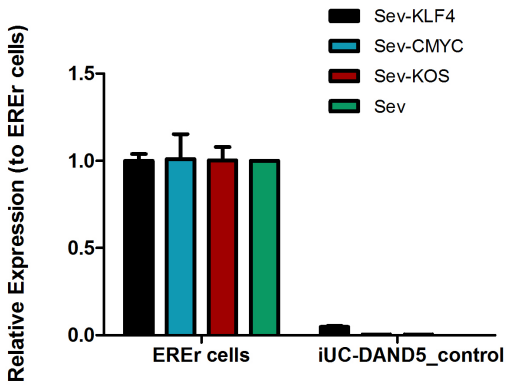

Figure 3.4. Transgene-free status of the established iPSC cell line. Absolute quantitative real-time PCR showing absence of the vectors and the exogenous reprogramming factor in iPSCs (right) and presence of the reprogramming factors in the EREr control cells (left).

3.5. *Mycoplasma*-free Culture

Mycoplasma species are known to be widely contaminating agents in cell cultures. They are hard to detect by visual identification due to their size and their contamination is problematic.

In order to detect the *Mycoplasma*-free status of the iPSCs culture, we performed a PCR experiment using two specific sets of primers that detect the *Mycoplasma* genes. The result showed no amplification in two independent Essential 8™ media samples (enumerated as 2 and 3 in Fig. 3.5 for each primer set) taken from different plates used for the culturing of the iPSC cells (Fig. 3.5). As a positive control for both primer sets,

cells known to be contaminated with *Mycoplasma* have been used. As negative control, we used the Essential 8™ media taken from the stock solution and incubated at 37°C with no cells.

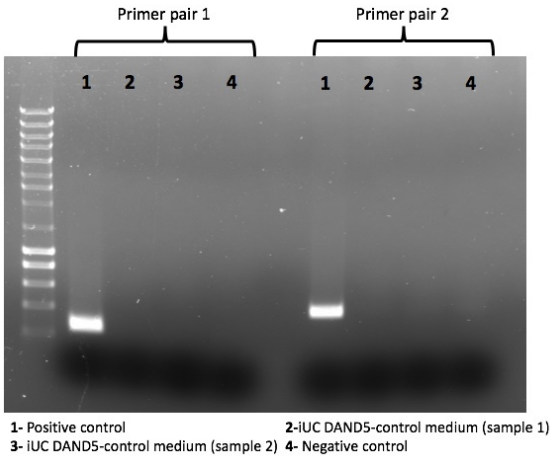

Figure 3.5. Mycoplasma contamination test. PCR showing the absence of Mycoplasma in the culture conditions of the iPSCs (1kb+ DNA Ladder was used as reference)**.**

3.6. Expression of Pluripotency Factors – Gene Level

The pluripotency factors are expressed solely by the pluripotent cells and are specific markers for those cells. Equally, the reprogramming of the cells does not occur naturally, therefore terminally differentiated cells are expected to have no significant expression of pluripotency genes in combination.

Therefore, the demonstration of expression of pluripotency factors in the induced PSCs are very crucial for their characterization.

To confirm the expression of pluripotency markers at mRNA level, gene expression analysis through quantitative RT-PCR was performed in the *DAND5*-control iPSC line.

According to our analysis (Fig. 3.6), the expression of the endogenous pluripotency genes *OCT3/4, NANOG, SOX2, KLF4* and *NODAL* in the established DAND5-control iPSC cell line is equal (*OCT4*) or higher (*NANOG, KLF4, SOX2, NODAL*) than the expression of those genes when in common human embryonic stem cells line (H9). Furthermore, these pluripotency genes were absent in exfoliated renal epithelial cells, except for *KLF4* that presents the same amount of expression in both cell lines.

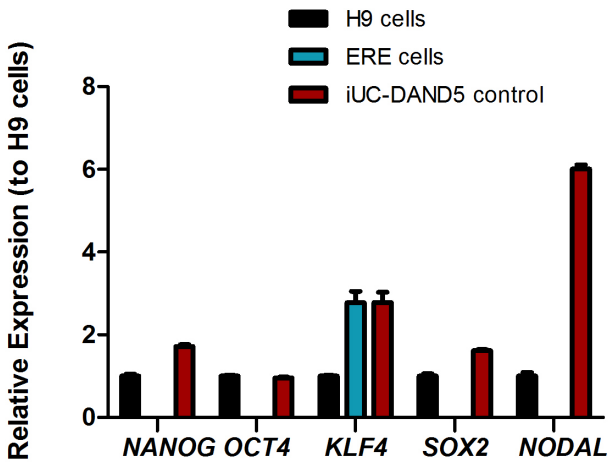

Figure 3.6. Relative expression of pluripotency genes *NANOG, OCT4 KLF4, SOX2*, and *NODAL*. mRNA expression levels of endogenous pluripotency markers in H9 cells (black - positive control), ERE cells (blue) and iUC-DAND5_455/control line (red).

3.7. Expression of Pluripotency Factors – Protein Level

In addition to the expression of pluripotency factors at mRNA level we also assessed the pluripotency state of the DAND5-control iPSC line at protein level. As we can see in the Fig. 3.7, immunofluorescence analysis confirmed the presence of NANOG, OCT4, and SSEA4, characteristic of pluripotent embryonic stem cells, in all cells from the colonies. OCT4 and NANOG are the self-renewal transcription markers, and hence are stained within the nuclei, whereas SSEA4 is a protein expressed at the plasma membrane, in concordance with its intercellular staining.

The expression of these proteins also illustrates the homogeneity and purity of the generated iPSC line.

Unstained cells are the dividing cells, as it can be seen with the DNA staining with DAPI.

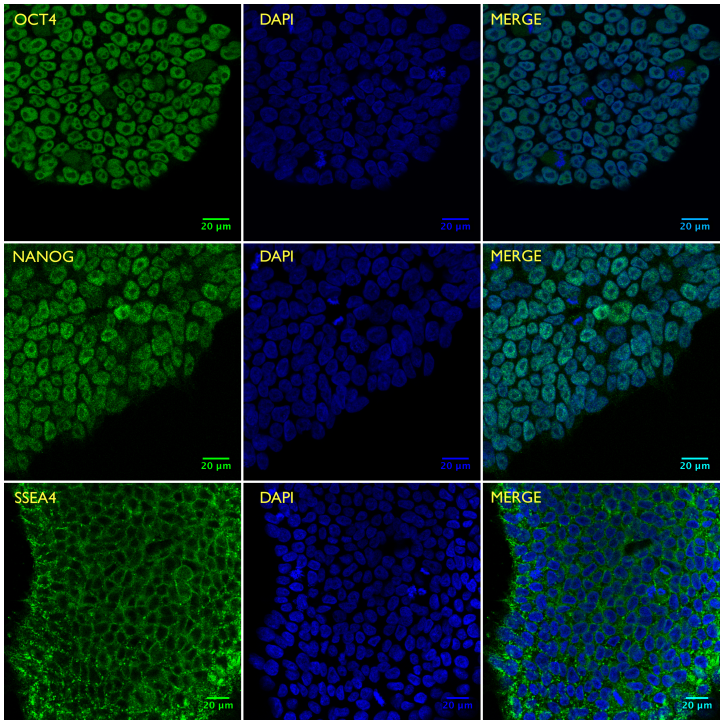

Fig. 3.7. Pluripotency of the *DAND5*-control cell line displayed at protein level. Immunofluorescence assay showing iPS cells positively stained with the pluripotency-associated markers OCT-4, NANOG, and SSEA4, proving the pluripotent state of the cell line. Images were acquired using Zeiss LSM710 confocal microscopy.

3.8. Differentiation Potential of iPSCs *in vitro*

Pluripotent stem cells are characterized by their potential to differentiate into the three germ layers that give rise to all the cells of the body; endoderm, ectoderm, and mesoderm. As pluripotent cells, iPSCs should be able to differentiate into all these three lineages.

To test the differentiation potential of our iPSCs, we used the hanging drop method to generate embryoid bodies, which allows the generation of cell clusters that are known to spontaneously differentiate in culture.

From this assay, we assessed that the EBs cultured for 19 days expressed markers of the three germ layers: endoderm, mesoderm, ectoderm, i.e., alpha-fetoprotein (AFP), smooth muscle actin (SMA), tubulin beta-3 chain (TUBB3), respectively (Fig. 3.8)

Each of the cover-slips were stained with different primary antibodies. Not all the cells in one single cluster expressed three germ layer markers. However, this is expected due to the spontaneous differentiation of the cells in vitro, where no specific differentiation was directed using any agent.

The result of this assay proved that the generated iPSCs can differentiate into three different cell types from three germ layers tested, which means they can differentiate into any cell type of the body.

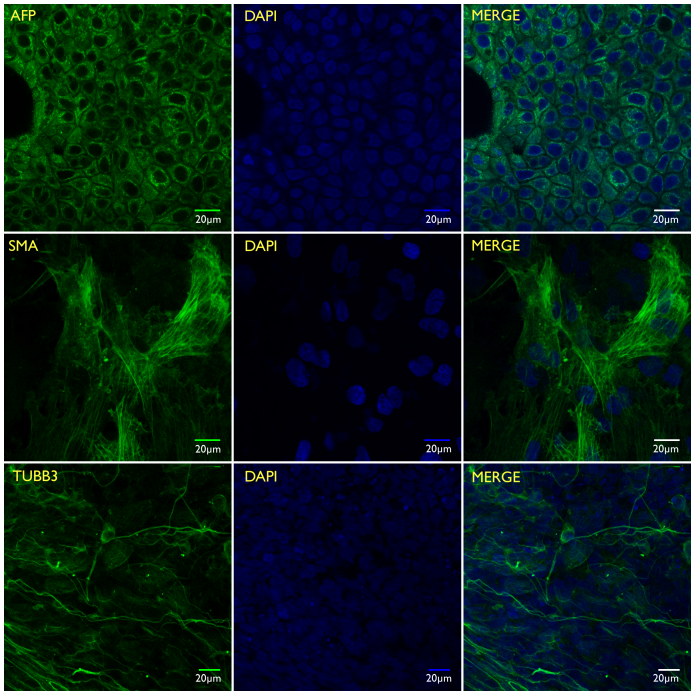

Figure 3.8. Spontaneous differentiation potential of iPSC *in vitro*. Immunofluorescence analyses of in vitro differentiation of EBs using specific antibodies against the endodermal marker α-fetoprotein (AFP), ectodermal marker βIII-tubulin (TUBB3) and mesodermal markers α-smooth muscle actin (SMA). Nuclei were stained with DAPI (scale bars=20µm).

3.9. Karyotype Analysis

The reprogramming, high proliferation rate and the relatively short doubling time of iPSCs increases the risk of chromosome instability. Therefore, to confirm that the iPSCs obtained through the transduction of the CytoTune® vectors, KOS (Klf4–Oct3/4–Sox2), hc-Myc, and hKlf4 into the renal epithelial cells maintain a proper genomic content, we performed the karyotype of the patient-derived iPSCs at passage 29. As presented in the Figure 3.9, the karyotype of the *DAND5*-control iPSCs seems to be normal, presenting 22 pairs of autosomal chromosomes and 1 pair of sex chromosomes. Nevertheless, a more detailed analysis of the chromosomes banding is currently ongoing to exclude possible subtle deletions, inversions, insertions, translocations, fragile sites and other more complex rearrangements.

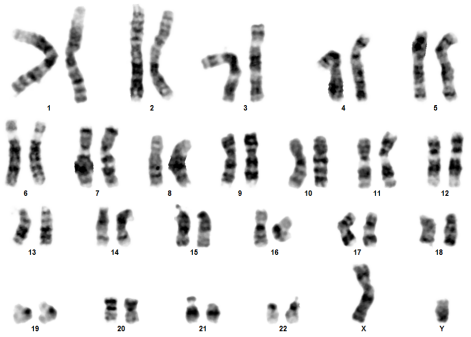

Fig. 3.9. Karyotype analysis of the iPSCs. Karyotype showing the normal 46, XX chromosomal arrangement of the *DAND5*-control iPSCs.

4. DISCUSSION AND CONCLUSIONS

TGF-ß/Nodal signalling pathway regulates the left-right axis establishment in vertebrates. The protein product of *Cerl2 gene* (*DAND5* in humans), being an antagonist in this pathway functions by binding to Nodal protein in the mice node.

The lack of this gene, studied in *Cerl2* knock-out (KO) mice results in laterality defects and a significant rate of mortality caused by cardiac defects (Marques *et al.*, 2004).

Additionally, *Cerl2* KO mice also display a massive increase of the ventricular cardiac walls due to an increased mitotic index of the cardiomyocytes, and more importantly from prolonged TGF-ß/Nodal signalling in those heart cells (Araujo, Marques & Belo, 2014).

The increased levels of nuclear ß-catenin in *Cerl2* KO mice also shows that the lack of *Cerl2* affects another pathway involved in cardiomyocyte proliferation. This finding shows that the lack of *Cerl2* in mice does not only cause laterality defects as previously thought, but also specifically regulates the cardiomyocyte proliferation through Wnt/ß-catenin and TGF-ß/Nodal signalling pathway.

In a previous study in our lab, that is the basis fort he work developed in this thesis, two patients were identified with a missense variant in the exon 2 of the *DAND5* genes (c.455G>A) (Cristo et al., 2017). Since an increase of the Nodal signalling was observed due to this variant, it was hypothesized, that similar to *Cerl2* KO mice, the cardiomyocyte proliferation and maturation could also be affected in these patients.

In order to test this hypothesis, the generation of a patient-specific *DAND5* human iPSC line, as well as a suitable related control one was undertaken. Therefore, in the work presented in this Master's thesis, a *DAND5*-control human iPSC line was characterized proving their transgene-free and pluripotent status, *in vitro* differential potential, and karyotype stability. The origin of the control cells was the ERE cells from a healthy male Caucasian without any alteration in *DAND5*. This donor is related to the patient that carries the *DAND5* variant c.455G>A.

An ideal control in this type of studies would be an isogenic cell line derived from the patient's own cells, since they have the same genotype as the patient, just mismatching in one nucleotide. Nerverthelese, the generation of an isogenic cell line was not possible by the time of this work. Moreover, in the future, and having this cell line characterized

we can induce the c.455G>A variant and clearly confirm the phenotype of those cells and exclude or not the action of other modifiers variants that the patient can have.

Although adult cardiac stem cells might be an alternative source to study the cardiac diseases, the amount of the cells obtained from patıents are very limited. Additionally, their isolation and expansion in the culture is not as easy as in iPSCs. Also, immature electrical phenotypes of the derived cells makes this application less effective.

In the future, the *DAND5* variant and the control cell line could be differentiated into cardiomyocytes, and subsequently, the proliferation rates of the ventricular cardiomyocytes could be investigated and compared *in vitro*. The establishment of this disease modelling at a later stage can be exploited for the discovery of the relevant drug candidates and serve for translational medicine purposes.

In spite of its promising potential, iPSC technology still is a recent methodology and its limitations need to be overcome. The improvement of new reprogramming methods that have higher reprogramming efficiency might accelerate the generation of iPSC from adult cells. Once reprogrammed, these cell should be expanded and mass produced for translational purposes.

Another hurdle that needs to be surpassed is to provide safety in case of the transplatation of cardiomyocytes. Reprogramming by the direct delivery of proteins or the avoidance of the use of viral methods would assure the safety requirements.

The differentiation of the iPSCs into the different subtypes of cardiomyocytes represents another limitation and the development of protocols to generate only specific subtypes of cardyomiıocytes need to be ensured to avoid the cardiac arrthymias caused by distinct beating patterns.

Other technologies such as heart-on-a-chip devices, that are mainly used in mimicing the cardiac tissue are also very promising approaches. The generation of iPSC and their subsequent differentiation into cardiomyocytes can provide a source as ‘bioink’ to 3D print a cardiac tissue.

Although the clinically approved therapies need to satisfy the requirements of the authorities, in the future, iPSC based therapies can be used as a personalized medicine approach that is essential to cure cardiovascular diseases, one of the major worldwide health problems.

5. BIBLIOGRAPHICAL REFERENCES

ABDULKADIR, Mohammed; ABDULKADIR, Zainab - A systematic review of trends and patterns of congenital heart disease in children in Nigeria from 1964-2015. **African Health Sciences**. . ISSN 16806905. (2016). doi: 10.4314/ahs.v16i2.5.

ABOU-SALEH, Haissam *et al.* - The march of pluripotent stem cells in cardiovascular regenerative medicine. **Stem cell research & therapy**. . ISSN 1757-6512. 9:1 (2018) 201. doi: 10.1186/s13287-018-0947-5.

AI, Di *et al.* - Pitx2 regulates cardiac left-right asymmetry by patterning second cardiac lineage-derived myocardium. **Developmental Biology**. . ISSN 00121606. (2006). doi: 10.1016/j.ydbio.2006.06.009.

ARAUJÓ, Ana Carolina; MARQUES, Sara; BELO, José António - Targeted inactivation of cerberus like-2 leads to left ventricular cardiac hyperplasia and systolic dysfunction in the mouse. **PLoS ONE**. . ISSN 19326203. 9:7 (2014). doi: 10.1371/journal.pone.0102716.

ÁVILA, Pablo *et al.* - Adult Congenital Heart Disease: A Growing Epidemic. **Canadian Journal of Cardiology**. . ISSN 0828282X. 30:12 (2014) S410–S419. doi: 10.1016/j.cjca.2014.07.749.

BEDDINGTON, Rosa S. P.; ROBERTSON, Elizabeth J. - Axis development and early asymmetry in mammals. **Cell**. . ISSN 00928674. 96:2 (1999) 195–209. doi: 10.1016/S0092-8674(00)80560-7.

CHAIX, Marie A. - Genetic testing in congenital heart disease: A clinical approach. **World Journal of Cardiology**. . ISSN 1949-8462. 8:2 (2016) 180. doi: 10.4330/wjc.v8.i2.180.

CHELO, David *et al.* - Spectrum of heart diseases in children: an echocardiographic study of 1,666 subjects in a pediatric hospital, Yaounde, Cameroon. **Cardiovascular diagnosis and therapy**. . ISSN 2223-3652. (2016). doi: 10.3978/j.issn.2223-3652.2015.11.04.

CRISTO, Fernando - **Molecular and functional analysis of DAND5 in human Congenital Heart Disease (CHD)**. Universidade do Algarve: Departamento de Ciências Biomédicas e Medicina - 2016. Tese de Doutoramento.

CRISTO, Fernando *et al.* - Functional study of DAND5 variant in patients with Congenital Heart Disease and laterality defects. **BMC Medical Genetics**. . ISSN

14712350. (2017). doi: 10.1186/s12881-017-0444-1.

CRISTO, Fernando *et al.* - Generation of human iPSC line from a patient with laterality defects and associated congenital heart anomalies carrying a DAND5 missense alteration. **Stem Cell Research**. . ISSN 18767753. (2017). doi: 10.1016/j.scr.2017.10.019.

DENG, Xia *et al.* - Characterization of Nodal/TGF-Lefty Signaling Pathway Gene Variants for Possible Roles in Congenital Heart Diseases. **PLoS ONE**. . ISSN 1932-6203. 9:8 (2014) e104535. doi: 10.1371/journal.pone.0104535.

DJORDJEVIC, Djordje *et al.* - Decoding the complex genetic causes of heart diseases using systems biology. **Biophysical Reviews**. . ISSN 1867-2450. 7:1 (2015) 141–159. doi: 10.1007/s12551-014-0145-3.

DUNN, Kaitlin K.; PALECEK, Sean P. - Engineering Scalable Manufacturing of High-Quality Stem Cell-Derived Cardiomyocytes for Cardiac Tissue Repair. **Frontiers in Medicine**. . ISSN 2296-858X. 5:April (2018). doi: 10.3389/fmed.2018.00110.

FERGUSON, Edwin L. - Conservation of dorsal ventral patterning in arthropods and chordates. **Current Opinion in Genetics and Development**. . ISSN 0959437X. 6:4 (1996) 424–431. doi: 10.1016/S0959-437X(96)80063-3.

FIXLER, D. E. *et al.* - Age at Referral and Mortality From Critical Congenital Heart Disease. **PEDIATRICS**. . ISSN 0031-4005. (2014). doi: 10.1542/peds.2013-2895.

FUJIE., Yasumitsu *et al.* - New type of sendai virus vector provides transgene-free iPS cells derived from chimpanzee blood. **PLoS ONE**. . ISSN 19326203. (2014). doi: 10.1371/journal.pone.0113052.

FUSAKI, Noemi *et al.* - Efficient induction of transgene-free human pluripotent stem cells using a vector based on Sendai virus, an RNA virus that does not integrate into the host genome. **Proceedings of the Japan Academy, Series B**. . ISSN 0386-2208. (2009). doi: 10.2183/pjab.85.348.

GILBOA, Suzanne M. *et al.* - Congenital Heart Defects in the United States: Estimating the Magnitude of the Affected Population in 2010. **Circulation**. . ISSN 15244539. (2016). doi: 10.1161/CIRCULATIONAHA.115.019307.

GITTENBERGER-DE GROOT, Adriana C. *et al.* - Basics of cardiac development for the understanding of congenital heart malformations. **Pediatric Research**. . ISSN 00313998. 57:2 (2005) 169–176. doi: 10.1203/01.PDR.0000148710.69159.61.

HAMADA, Hiroshi *et al.* - Establishment of vertebrate left-right asymmetry. **Nature**

Reviews Genetics. . ISSN 14710056. 3:2 (2002) 103–113. doi: 10.1038/nrg732.

HAMADA, Hiroshi; TAM, Patrick P. L. - Mechanisms of left-right asymmetry and patterning: driver, mediator and responder. **F1000Prime Reports**. . ISSN 20517599. (2014). doi: 10.12703/P6-110.

HILL, Caroline S. - Spatial and temporal control of NODAL signaling. **Current Opinion in Cell Biology**. . ISSN 18790410. (2018). doi: 10.1016/j.ceb.2017.10.005.

HIROKAWA, Nobutaka; TANAKA, Yosuke; OKADA, Yasushi - Left-right determination: involvement of molecular motor KIF3, cilia, and nodal flow. **Cold Spring Harbor perspectives in biology**. . ISSN 19430264. (2009). doi: 10.1101/cshperspect.a000802.

INÁCIO, José Manuel *et al.* - The Dynamic Right-to-Left Translocation of Cerl2 Is Involved in the Regulation and Termination of Nodal Activity in the Mouse Node. **PLoS ONE**. . ISSN 19326203. 8:3 (2013). doi: 10.1371/journal.pone.0060406.

KAVYASUDHA, Chavali *et al.* - Clinical Applications of Induced Pluripotent Stem Cells - Stato Attuale. **Advances in experimental medicine and biology**. . ISSN 0065-2598. (2018). doi: 10.1007/5584_2018_173.

KUMAR V, ABBAS AK, Aster JC - Basic Pathology. Em **Robbins Basic Pathology 9th Edition**. ISBN 1-4160-2973-7

LEVIN, Michael - Left-right asymmetry in embryonic development: A comprehensive review. **Mechanisms of Development**. . ISSN 09254773. (2005). doi: 10.1016/j.mod.2004.08.006.

LI, Nana *et al.* - Assessment of interaction between maternal polycyclic aromatic hydrocarbons exposure and genetic polymorphisms on the risk of congenital heart diseases. **Scientific Reports**. . ISSN 20452322. 8:1 (2018) 1–13. doi: 10.1038/s41598-018-21380-3.

LIN, Angela E. *et al.* - Laterality defects in the national birth defects prevention study (1998-2007): Birth prevalence and descriptive epidemiology. **American Journal of Medical Genetics, Part A**. . ISSN 15524833. (2014). doi: 10.1002/ajmg.a.36695.

LINDE, Denise VAN DER *et al.* - Birth prevalence of congenital heart disease worldwide: A systematic review and meta-analysis. **Journal of the American College of Cardiology**. . ISSN 07351097. (2011). doi: 10.1016/j.jacc.2011.08.025.

LIU, C. *et al.* - Regulation of left-right asymmetry by thresholds of Pitx2c activity.

Development (Cambridge, England). . ISSN 0950-1991. (2001). doi: 10.1073/pnas.95.8.4573.

MARQUES, Sara *et al.* - The activity of the Nodal antagonist. **Genes & Development**. . ISSN 08909369. (2004) 2342–2347. doi: 10.1101/gad.306504.2342.

MCNAMARA-SCHROEDER, Kathleen *et al.* - DNA fingerprint analysis of three short tandem repeat (STR) loci for biochemistry and forensic science laboratory courses. **Biochemistry and Molecular Biology Education**. . ISSN 1470-8175. 34:5 (2006) 378–383. doi: 10.1002/bmb.2006.494034052665.

MEINHARDT, Hans - Dorsoventral patterning by the Chordin-BMP pathway: A unified model from a pattern-formation perspective for drosophila, vertebrates, sea urchins and nematostella. **Developmental Biology**. . ISSN 1095564X. 405:1 (2015) 137–148. doi: 10.1016/j.ydbio.2015.05.025.

MOHAPATRA, Bhagyalaxmi *et al.* - Identification and functional characterization of NODAL rare variants in heterotaxy and isolated cardiovascular malformations. **Human Molecular Genetics**. . ISSN 09646906. (2009). doi: 10.1093/hmg/ddn411.

MOONS, Philip *et al.* - Structure and activities of adult congenital heart disease programmes in Europe. **European Heart Journal**. . ISSN 0195668X. 31:11 (2010) 1305–1310. doi: 10.1093/eurheartj/ehp551.

MOORE, Keith L.; PERSAUD, T. V. N.; TORCHIA, Mark G. - **The Developing Human**. ISBN 0721694128.

MOORMAN, A. - Development of the Heart: (1) Formation of the Cardiac Chambers and Arterial Trunks. **Heart**. . ISSN 0007-0769. 89:7 (2003) 806–814. doi: 10.1136/heart.89.7.806.

MORRIS, Samantha A. *et al.* - Dynamics of anterior-posterior axis formation in the developing mouse embryo. **Nature Communications**. . ISSN 20411723. 3: (2012) 610–673. doi: 10.1038/ncomms1671.

MUSUMECI, Giuseppe *et al.* - Somitogenesis: From somite to skeletal muscle. **Acta Histochemica**. . ISSN 16180372. 117:4–5 (2015) 313–328. doi: 10.1016/j.acthis.2015.02.011.

NAGASAKA, Risako *et al.* - Visualization of morphological categories of colonies for monitoring of effect on induced pluripotent stem cell culture status. **Regenerative Therapy**. . ISSN 23523204. 6: (2017) 41–51. doi: 10.1016/j.reth.2016.12.003.

NONAKA, Shigenori *et al.* - Randomization of left-right asymmetry due to loss of nodal cilia generating leftward flow of extraembryonic fluid in mice lacking KIF3B motor protein. **Cell**. . ISSN 00928674. 95:6 (1998) 829–837. doi: 10.1016/S0092-8674(00)81705-5.

OKI, S. *et al.* - Reversal of left-right asymmetry induced by aberrant Nodal signaling in the node of mouse embryos. **Development**. . ISSN 0950-1991. (2009). doi: 10.1242/dev.039305.

PATEL, Ketan; ISAAC, Alison; COOKE, Jonathan - Nodal signalling and the roles of the transcription factors SnR and Pitx2 in vertebrate left-right asymmetry. **Current Biology**. . ISSN 09609822. (1999). doi: 10.1016/S0960-9822(99)80267-X.

RAAB, Stefanie *et al.* - A Comparative View on Human Somatic Cell Sources for iPSC Generation. **Stem Cells International**. . ISSN 16879678. (2014). doi: 10.1155/2014/768391.

RAMAKRISHNAN, Anushuya *et al.* - Maternal Hypertension During Pregnancy and the Risk of Congenital Heart Defects in Offspring: A Systematic Review and Meta-analysis. **Pediatric Cardiology**. . ISSN 14321971. (2015). doi: 10.1007/s00246-015-1182-9.

RAMSDELL, Ann F. - Left-right asymmetry and congenital cardiac defects: Getting to the heart of the matter in vertebrate left-right axis determination. **Developmental Biology**. . ISSN 00121606. (2005). doi: 10.1016/j.ydbio.2005.07.038.

RAYA, Ángel; IZPISÚA BELMONTE, Juan Carlos - Left-right asymmetry in the vertebrate embryo: From early information to higher-level integration. **Nature Reviews Genetics**. . ISSN 14710056. 7:4 (2006) 283–293. doi: 10.1038/nrg1830.

ROODE, Mila *et al.* - Human hypoblast formation is not dependent on FGF signalling. **Developmental Biology**. . ISSN 1095564X. (2012). doi: 10.1016/j.ydbio.2011.10.030.

SAIJOH, Yukio *et al.* - Left-right patterning of the mouse lateral plate requires Nodal produced in the node. **Developmental Biology**. . ISSN 00121606. (2003). doi: 10.1016/S0012-1606(02)00121-5.

SÁNCHEZ-QUINTANA, Damián; YEN HO, Siew - Anatomy of cardiac nodes and atrioventricular specialized conduction system. **Revista espanola de cardiologia**. . ISSN 0300-8932. (2003). doi: 13054255 [pii].

SCHLEICH, Jean Marc *et al.* - An overview of cardiac morphogenesis. **Archives of Cardiovascular Diseases**. . ISSN 18752136. 106:11 (2013) 612–623. doi:

10.1016/j.acvd.2013.07.001.

SHAO, Lijian; WU, Wen-Shu - Gene-delivery systems for iPS cell generation. **Expert Opinion on Biological Therapy**. . ISSN 1471-2598. (2010). doi: 10.1517/14712590903455989.

SHEN, M. M. - Nodal signaling: developmental roles and regulation. **Development**. . ISSN 0950-1991. (2007). doi: 10.1242/dev.000166.

SHIRATORI, Hidetaka; HAMADA, Hiroshi - TGFβ signaling in establishing left-right asymmetry. **Seminars in Cell and Developmental Biology**. . ISSN 10963634. 32:(2014) 80–84. doi: 10.1016/j.semcdb.2014.03.029.

SIEBER-BLUM, Maya - Cardiac neural crest stem cells. **The Anatomical Record**. . ISSN 0003-276X. 276A:1 (2004) 34–42. doi: 10.1002/ar.a.10132.

SILVA, Juneo F.; SERAKIDES, Rogéria - Intrauterine trophoblast migration: A comparative view of humans and rodents. **Cell Adhesion and Migration**. . ISSN 19336926. 10:1–2 (2016) 88–110. doi: 10.1080/19336918.2015.1120397.

SINGH, Vimal K. *et al.* - Induced pluripotent stem cells: applications in regenerative medicine, disease modeling, and drug discovery. **Frontiers in Cell and Developmental Biology**. . ISSN 2296-634X. 3:February (2015) 1–18. doi: 10.3389/fcell.2015.00002.

SMITH, Kelly A. *et al.* - Bmp and Nodal independently regulate lefty1 expression to maintain unilateral Nodal activity during left-right axis specification in zebrafish. **PLoS Genetics**. . ISSN 15537390. (2011). doi: 10.1371/journal.pgen.1002289.

SRINIVAS, S. - Active cell migration drives the unilateral movements of the anterior visceral endoderm. **Development**. . ISSN 0950-1991. 131:5 (2004) 1157–1164. doi: 10.1242/dev.01005.

STADTFELD, Matthias; HOCHEDLINGER, Konrad - Induced pluripotency: history, mechanisms, and applications. **Genes & development**. . ISSN 1549-5477. (2010) 2239–2263. doi: 10.1101/gad.1963910.Freely.

SUN, Cheng; KONTARIDIS, Maria I. - Physiology of cardiac development: from genetics to signaling to therapeutic strategies. **Current Opinion in Physiology**. . ISSN 24688673. (2018). doi: 10.1016/j.cophys.2017.09.002.

SUN, Ning *et al.* - Patient-specific induced pluripotent stem cells as a model for familial dilated cardiomyopathy. **Science Translational Medicine**. . ISSN 19466234. (2012). doi: 10.1126/scitranslmed.3003552.

SUN, RongRong *et al.* - Congenital Heart Disease: Causes, Diagnosis, Symptoms, and Treatments. **Cell Biochemistry and Biophysics**. . ISSN 1085-9195. 72:3 (2015) 857–860. doi: 10.1007/s12013-015-0551-6.

SYLVA, Marc; HOFF, Maurice J. B. VAN DEN; MOORMAN, Antoon F. M. - Development of the human heart. **American Journal of Medical Genetics, Part A**. . ISSN 15524833. 164:6 (2014) 1347–1371. doi: 10.1002/ajmg.a.35896.

TAKAHASHI, Kazutoshi *et al.* - Induction of Pluripotent Stem Cells from Adult Human Fibroblasts by Defined Factors. **Cell**. . ISSN 00928674. 131:5 (2007) 861–872. doi: 10.1016/j.cell.2007.11.019.

TAKAHASHI, Kazutoshi; YAMANAKA, Shinya - Induction of Pluripotent Stem Cells from Mouse Embryonic and Adult Fibroblast Cultures by Defined Factors. **Cell**. . ISSN 00928674. (2006). doi: 10.1016/j.cell.2006.07.024.

THOMSON, J. A. - Embryonic Stem Cell Lines Derived from Human Blastocysts. **Science**. . ISSN 0036-8075. (1998). doi: 10.1126/science.282.5391.1145.

TOMANEK, Robert J. - Formation of the coronary vasculature during development. **Angiogenesis**. . ISSN 09696970. (2005). doi: 10.1007/s10456-005-9014-9.

VERSACCI, Paolo *et al.* - Some Isolated Cardiac Malformations Can Be Related to Laterality Defects. . ISSN 2308-3425. (2018). doi: 10.3390/jcdd5020024.

VETRINI, Francesco *et al.* - Bi-allelic Mutations in PKD1L1 Are Associated with Laterality Defects in Humans. **American Journal of Human Genetics**. . ISSN 15376605. 99:4 (2016) 886–893. doi: 10.1016/j.ajhg.2016.07.011.

WAKAO, Shohei *et al.* - Morphologic and Gene Expression Criteria for Identifying Human Induced Pluripotent Stem Cells. **PLoS ONE**. . ISSN 19326203. 7:12 (2012). doi: 10.1371/journal.pone.0048677.

WANG, Gang *et al.* - Modeling the mitochondrial cardiomyopathy of Barth syndrome with induced pluripotent stem cell and heart-on-chip technologies. **Nature Medicine**. . ISSN 1546170X. (2014). doi: 10.1038/nm.3545.

YA, Jing *et al.* - Expression of the smooth-muscle proteins α-smooth-muscle actin and calponin, and of the intermediate filament protein desmin are parameters of cardiomyocyte maturation in the prenatal rat heart. **Anatomical Record**. . ISSN 0003276X. 249:4 (1997) 495–505. doi: 10.1002/(SICI)1097-0185(199712)249:4<495::AID-AR9>3.0.CO;2-Q.

YAMANAKA, Shinya; BLAU, Helen M. - Nuclear reprogramming to a pluripotent state by three approaches. **Nature**. . ISSN 00280836. (2010). doi: 10.1038/nature09229.

YU, Junying *et al.* - Induced pluripotent stem cell lines derived from human somatic cells. **Science (New York, N.Y.)**. . ISSN 1095-9203. (2007). doi: 10.1126/science.1151526.

ZHAO, Jing *et al.* - Induced pluripotent stem cells: origins, applications, and future perspectives. **Journal of Zhejiang University SCIENCE B**. . ISSN 1673-1581. (2013). doi: 10.1631/jzus.B1300215.

ZHOU, X. *et al.* - Nodal is a novel TGF-beta-like gene expressed in the mouse node during gastrulation. **Nature**. . ISSN 0028-0836. 361:6412 (1993) 543–547. doi: 10.1038/361543a0.

ZINSKI, Joseph; TAJER, Benjamin; MULLINS, Mary C. - TGF- b Family Signaling in Early Vertebrate Development. **Cold Spring Harbor Perspectives in Biology**. . ISSN 1943-0264. (2017) 1–76. doi: 10.1101/cshperspect.a022152.

6. ATTACHMENTS

ANNEX I

1. PCR conditions of the *DAND5* exon 2 amplification:

DAND5:

98°C 1:00 min. x1
98°C 00:15 min.
65°C 00:25 min.
72°C 00:20 min. x35
72°C 00:30 min.

2. cDNA Synthesis Protocol

1. Defrost the components of the RevertAid First Strand cDNA Synthesis Kit oligodT, RT Buffer, RiboLock, dNTPS (10mM) and the RNA samples.

2. Prepare the PCR tubes, and add the relevant amounts of RNA, oligodT, and nuclease free (NF) water.

The total amount of the mix should be 12,5 µl (1µl oligodT + 1000ng RNA + NF water).

3. Incubate the PCR tubes at 65°C for 5 minutes. After 5 minutes, place the samples immediately on ice (or set 12°C after the first step in thermal cycler instrument).

4. Calculate the master mix amount you need and prepare it in a 1,5ml microcentrifuge tube according to the table below:

RT Buffer	4 µl
RiboLock	0,5 µl
dNTP	2 µl
RT enzyme	1 µl
Total (per sample):	7,5 µl

5. Pipette 7,5µl of the master mix to each sample (the final amount will thus be 20 µl per sample) and start the PCR reaction at 42°C according to the temperatures below:

65°C 5:00 min. 1x
12°C ∞ 1x
42°C 60:00 min.
72°C 5:00 min.
12°C ∞ 1x

6. After the reaction terminates, label the PCR tubes and store the cDNAs in -20°C.

ANNEX II

RT-qPCR Protocol

1. Defrost SYBR Green (once thawed, protect from the light), primer pairs, and the cDNAs, place on ice.

2. Calculate the qPCR mix amount you need **per primer pair** and prepare it in a 1,5ml microcentrifuge tube according to the table (amounts per sample) below:

SYBR Green	7,5 µl
Forward Primer	1,0 µl
Reverse Primer	1,0 µl
H_2O	3,5 µl
Total:	13 µl

The list of controls:
Positive control: H9 commercial stem cell line
Negative control: Exfoliated renal epithelial (ERE) cells
qPCR control: qPCR mix without the cDNA (NF H2O instead)

3. Label the corners of the qPCR plate according to the gene name tested.

4. Pipette 13µl of qPCR mix with the relevant primers in each well (you may want to use triplicates). Pipette them at the bottom of the wells.

5. Pipette 2µl of cDNA at the corners of the well.

6. Centrifuge the qPCR plate for 1 min. at 1,200 rpm.

7. Place the qPCR plate in the instrument, set up the conditions and start the experiment according to the list below:

PCR conditions of the pluripotency and the house-keeping genes:
NANOG, OCT3/4, ß-ACTIN:

95°C 10:00 min. x1
95°C 00:30 min.

55°C 00:15 min.
72°C 00:30 min. x40

hSOX2, hNODAL, KLF-4:

95°C 10:00 min. x1
95°C 00:30 min.
65°C 00:15 min.
72°C 00:30 min. x40

GAPDH:

95°C 10:00 min. x1
95°C 00:30 min.
61,3°C 00:15 min.
72°C 00:30 min. x40

ANNEX III

Table 1.1. Antibodies used in immunocytochemistry assay

Antibody	Marker Type	Dilution	Information
Rabbit anti-NANOG	Pluripotency	1:200	Abcam Cat# ab21624, RRID:AB_446437
Rabbit anti-OCT4	Pluripotency	1:400	Abcam Cat# ab19857, RRID:AB_445175
Mouse anti-SSEA4	Pluripotency	1:200	Abcam Cat# ab16287, RRID:AB_778073
Mouse anti-Human TUBB3	Differentiation (ectoderm)	1:400	Sigma-Aldrich Cat# T8660, RRID:AB_477590
Mouse anti-Human SMA	Differentiation (mesoderm)	1:600	Dako Cat# M0851, RRID:AB_2223500
Rabbit anti-Human AFP	Differentiation (endoderm)	1:200	Dako Cat# A0008, RRID:AB_2650473
Alexa Fluor 488-conjugated Donkey anti-Mouse IgG (H + L)	Secondary Antibody	1:300	Jackson ImmunoResearch Labs Cat# 715-545-150, RRID:AB_2340846
Alexa Fluor 488-conjugated Donkey anti-Rabbit IgG (H + L)	Secondary Antibody	1:300	Jackson ImmunoResearch Labs Cat# 711-545-152, RRID:AB_2313584

Table 1.2. Primer sequences of Pluripotency Genes and House-keeping Genes

Gene	Forward Primer (5'-3')	Reverse Primer (5'-3')
NANOG	CATGAGTGTGGATCCAGCTTG	CCTGAATAAGCAGATCCATGG
OCT3/4	GACAGGGGGAGGGGAGGAGCTAGG	CTTCCCTCCAACCAGTTGCCCCAAAC
KLF-4	ACCAGGCACTACCGTAAACACA	GGTCCGACCTGGAAAATGCT
SOX2	GGGAAATGGGAGGGGTGCAAAAGAGG	TTGCGTGAGTGTGGATGGGATTGGTG
NODAL	GGGCAAGAGGCACCGTCGACATCA	GGGACTCGGTGGGGCTGGTAACGTTTC
GAPDH	CTGGTAAAGTGGATATTGTTGCCAT	TGGAATCATATTGGAACATGTAAACC
ß-ACTIN	GCAAAGACCTGTACGCCAAC	AGTACTTGCGCTCAGGAGGA

Table 1.3. Primer sequences of Sendai-virus specific genes

Gene	Forward Primer (5'-3')	Reverse Primer (5'-3')
SeV	GGATCACTAGGTGATATCGAGC	ACCAGACAAGAGTTTAAGAGATATGTATC
Sev-KLF4	TTCCTGCATGCCAGAGGAGCCC	AATGTATCGAAGGTGCTCAA
Sev-C-MYC	TAACTGACTAGCAGGCTTGTCG	TCCACATACAGTCCTGGATGATGATG
Sev-KOS	ATGCACCGCTACGACGTGAGCGC	ACCTTGACAATC CTGATGTGG

Table 1.4. Primer sequences of *DAND5* exon 2

Gene	Forward Primer (5'-3')	Reverse Primer (5'-3')
DAND5 exon 2	GGAAGTGGACAGGTGATTATCC	CACGTCTTTCTTGGTCCATCTC

Table 1.5. Primer sequences of *Mycoplasma*

Gene	Forward Primer (5'-3')	Reverse Primer (5'-3')
Pair 1	CTGCAGATTGCAAAGCAAGA	CCTCCTTCTTCACCTGCTTG
Pair 2	GGCGAATGGGTGAGTAACACG	CGGATAACGCTTGCGACCTATG